Special Isotopes of the FUGEN Nuclear Reactor

by

Timothy R. Davis

A thesis submitted to the School of Graduate and
Postdoctoral Studies in partial fulfilment of the
requirements for the degree of

Master of Applied Science in Nuclear Engineering

Faculty of Energy Systems and Nuclear Science

University of Ontario Institute of Technology (Ontario Tech University)

Oshawa, Ontario, Canada

April 2022

THESIS EXAMINATION INFORMATION

Submitted by: **Timothy Davis**

Masters of Applied Science in **Nuclear Engineering**

Thesis title: Special Isotopes of the FUGEN Nuclear Reactor

An oral defence of this thesis took place on March 21, 2022 in front of the following examining committee:

Examining Committee:

Chair of Examining Committee	Dr. Jennifer McKellar
Research Supervisor	Dr. Edward Waller
Examining Committee Member	Dr. Scott Nokleby
Thesis Examiner	Dr. Brian Ikeda, Ontario Tech University

The above committee determined that the thesis is acceptable in form and content and that a satisfactory knowledge of the field covered by the thesis was demonstrated by the candidate during an oral examination. A signed copy of the Certificate of Approval is available from the School of Graduate and Postdoctoral Studies.

ABSTRACT

The Canadian and Japanese nuclear regulatory bodies have shown dissimilarities between the isotopes considered to be of interest in decommissioning similarly styled heavy water reactors. This research examines the quantity of the isotopes that are of interest to the decommissioning of both the FUGEN nuclear power plant in Japan and the Pickering nuclear power plant in Canada and makes a comparison between them. This comparison is accomplished by modeling the fuel assemblies of both reactors in MCNP and performing depletion calculations on them to calculate the type and quantity of the produced fission and activation products, after which ratio comparisons are made between reactors. The FUGEN fuel has shown a greater isotope production than Pickering when normalized to fuel volume, with isotopes in FUGEN showing up to forty-five times the concentration when compared per unit volume with many isotopes produced in FUGEN not appearing in Pickering at all.

Keywords: MCNP; Decommissioning; Pickering; Fugen; Isotopes

AUTHOR'S DECLARATION

I hereby declare that this thesis consists of original work of which I have authored. This is a true copy of the thesis, including any required final revisions, as accepted by my examiners.

I authorize the University of Ontario Institute of Technology (Ontario Tech University) to lend this thesis to other institutions or individuals for the purpose of scholarly research. I further authorize University of Ontario Institute of Technology (Ontario Tech University) to reproduce this thesis by photocopying or by other means, in total or in part, at the request of other institutions or individuals for the purpose of scholarly research. I understand that my thesis will be made electronically available to the public.

_____ Timothy Davis

STATEMENT OF CONTRIBUTIONS

I hereby certify that I am the sole author of this thesis and that no part of this thesis has been published or submitted for publication. I have used standard referencing practices to acknowledge ideas, research techniques, or other materials that belong to others. Furthermore, I hereby certify that I am the sole source of the creative works and/or inventive knowledge described in this thesis.

ACKNOWLEDGEMENTS

I would like to thank my supervisor Dr. Edward Waller as well as Dr. Scott Nokleby and Dr. Brian Ikeda for their guidance on this project as well as Dr. Glenn Harvel for providing data as well as the original idea for the project. Additionally I would like to thank my colleague Nicholas Somer for some of his insights on the origins of the isotopes of interest.

Contents

List of Tables

List of Figures

List of Abbreviations

3D = Three-Dimensional

(n,γ) = Neutron-Gamma Reaction

(n,α) = Neutron-Alpha Reaction

(n,β) = Neutron-Beta Reaction

(n,p) = Neutron-Proton Reaction

(n,f) = Neutron-Fission Reaction

(n,f) = Neutron-Fission Reaction

AECL = Atomic Energy of Canada Limited

ATR = Advanced Thermal Reactor

CAD = Computer-Aided Design

CANDU = Canada Deuterium Uranium

EQ = Exemption Quantity

FSD = Fractional Standard Deviation

IAEA = International Atomic Energy Agency

JAEA = Japanese Atomic Energy Agency

k$_{eff}$ = K-effective

MCNP = Monte Carlo N-Particle

MOX = Mixed Oxide

nUO$_2$ = Natural Uranium Dioxide

RCC = Right Circular Cylinder

UCL = Unconditional Clearance Limit

Chapter 1

Background and Motivation

1.1 Purpose of Research

Decommissioning refers to the processes undergone in order to put nuclear plants out of service. The Pickering CANDU reactors in Canada will be undergoing decommissioning in the upcoming years. Comparing the isotopes of interest produced within the Pickering reactor to those of the FUGEN reactor being decommissioned in Japan should help inform decisions made regarding the decommissioning of the Pickering reactors as both are heavy-water moderated.

A greater understanding of the safety measures required to decommission these reactors is ascertained by examining the differences in isotopic content between these reactors. As the information on the isotopic inventories of the FUGEN reactor is not readily available, models are necessary to understand the regulator's view on

why certain isotopes are of interest. These models will help in understanding isotope production in the different types of heavy-water reactors. These models will show the direct production of these "special" isotopes or their precursor isotopes, which can be activated to become them.

Both nations that regulate these reactors comply with the International Atomic Energy Agency (IAEA) guidelines. Therefore they should have similar regulations and standards for the allowable concentrations of these isotopes regarding decommissioning based on the IAEA guidelines for clearance levels of radioactive materials as well as the classifications of radioactive waste (*Application of the Concepts of Exclusion, Exemption and Clearance*, 2004; *Classification of Radioactive Waste*, 2009). Due to this, if an isotope is determined to be of interest to one regulatory body and not the other, it should be due to radiological differences, not regulatory distinctions. Based on this, this research will work toward modelling the fuel of the FUGEN and Pickering models and comparing the generated isotopic inventories of each reactor in order to explain why these isotopes are of interest to one country and not the other based on the radiological differences.

1.2 The FUGEN Nuclear Reactor of Japan

FUGEN, the Advanced Thermal Reactor (ATR) located in Tsuruga, Japan was the first thermal reactor to demonstrate the full-scale utilization of uranium-plutonium mixed oxide (MOX) fuel assemblies in the world and played a leading role in plutonium utilization during its approximately 25 year operation period running from 1979 to

2003 (Sawai, Haga, Akebi, & Kontani, 1979). While in operation, FUGEN produced 165 MW of electrical output, making it the smallest of the Japanese nuclear power plants. The basic design of the FUGEN reactor core and cooling can be seen in Figure 1.1 (FUGEN Decommissioning Engineering Center, 2015, para.11).

Figure 1.1:

FUGEN Reactor Core and Cooling Systems

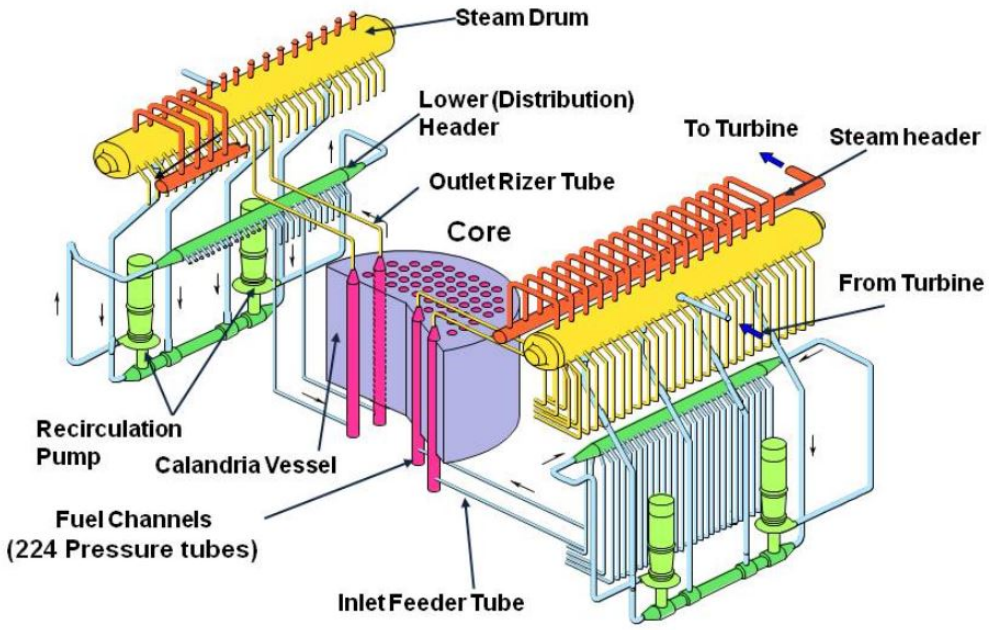

Note. The cross-section of the reactor core and cooling systems of the FUGEN reactor. From FUGEN Decommissioning Engineering Center (2015, para.11). Copyright 2015 by Fugen Decommissioning Engineering Center. JAEA All Rights Reserved.

FUGEN was a heavy-water moderated, boiling light-water cooled, pressure tube reactor. The reactor consisted of a calandria tank, pressure tubes, control rods, fuel rods, iron and water shields, pumps, turbines and many other components. The reactor core data is shown in Table 1.1 (Ohtani, Iijima, & Shiratori, 2003, p.959).

Table 1.1:

FUGEN Reactor Core Data

Item	Specification
Reactor type	heavy-water moderated, light-water cooled
Thermal output	557 MW
Electrical output	165 MW
Core height	3.7 m
Core diameter	4.05 m
Coolant pressure	68 kg/cm^{2}a
Coolant flow rate	7600 t/h
Number of fuel assemblies	224
Number of control rods	49
Moderator (D2O) inventory	160 t

Note. Reactor data for the FUGEN nuclear reactor in Japan. From Ohtani et al. (2003, p.959). Copyright 2003 by Taylor and Francis.

The 224 pressure tubes were installed vertically in the heavy-water moderated calandria tank. A fuel assembly was installed in each pressure tube, around which light-water flowed as coolant. Both the coolant and moderator were pumped into the reactor through inlets below the reactor and forced to flow vertically upward. A cross-section of a pressure tube can be seen in Figure 1.2 (Ohtani et al., 2003, p.963).

Figure 1.2:

Cross-Section of FUGEN Reactor Fuel Channel

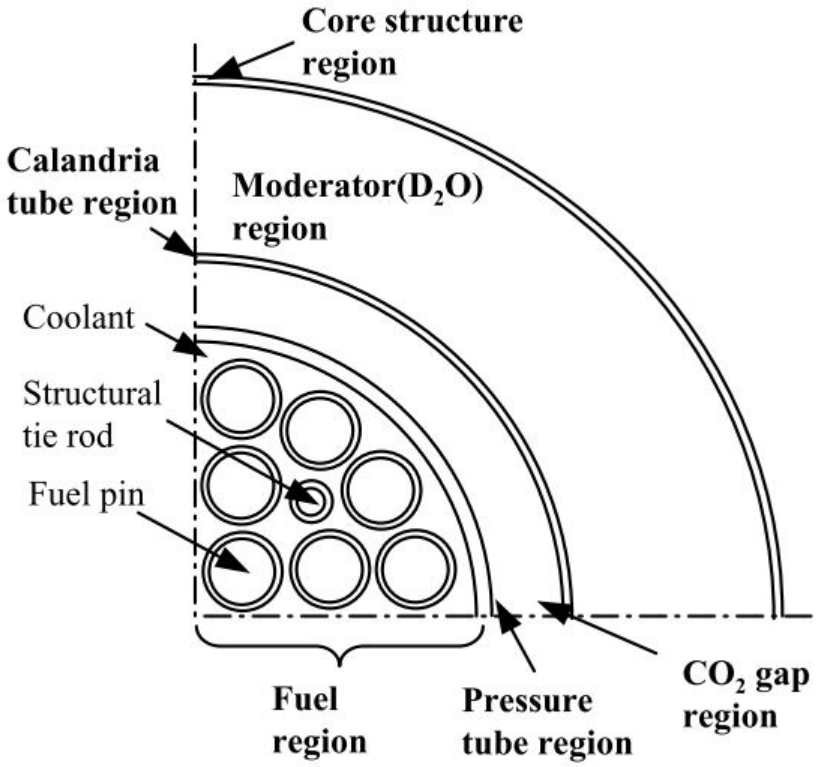

Note. The cross-section of the FUGEN reactors fuel showing different regions of the calandria tube. From Ohtani et al. (2003, p.963). Copyright 2003 by Taylor and Francis.

The 49 control rods were inserted from the reactor top into the heavy-water via guide tubes installed in the calandria tank. ^{10}B was added to the heavy-water to control burnup reactivity in the core. A cross-section of the reactor core can be seen in Figure 1.3 (FUGEN Decommissioning Engineering Center, 2015, para.11). In this cross-section it can be seen that the FUGEN reactor used heavy-water as a moderator, with carbon dioxide used as an annulus gas separating the coolant channel and the calandria tubes. A typical core layout of a fuel assembly can be seen in Figure 1.4

(Ohtani et al., 2003, p.962). The FUGEN reactor used a combination of MOX and slightly enriched UO_2. While the concentrations of UO_2 and PuO_2 vary based on placement within the reactor core, typical average concentrations found in the fuel are 1.5% ^{235}U and 0.66% plutonium enrichment (Kato & Miyawaki, 1976). The derivations and use of these concentrations will be described further in the methodology section.

Figure 1.3:

Cross-Section of FUGEN Core

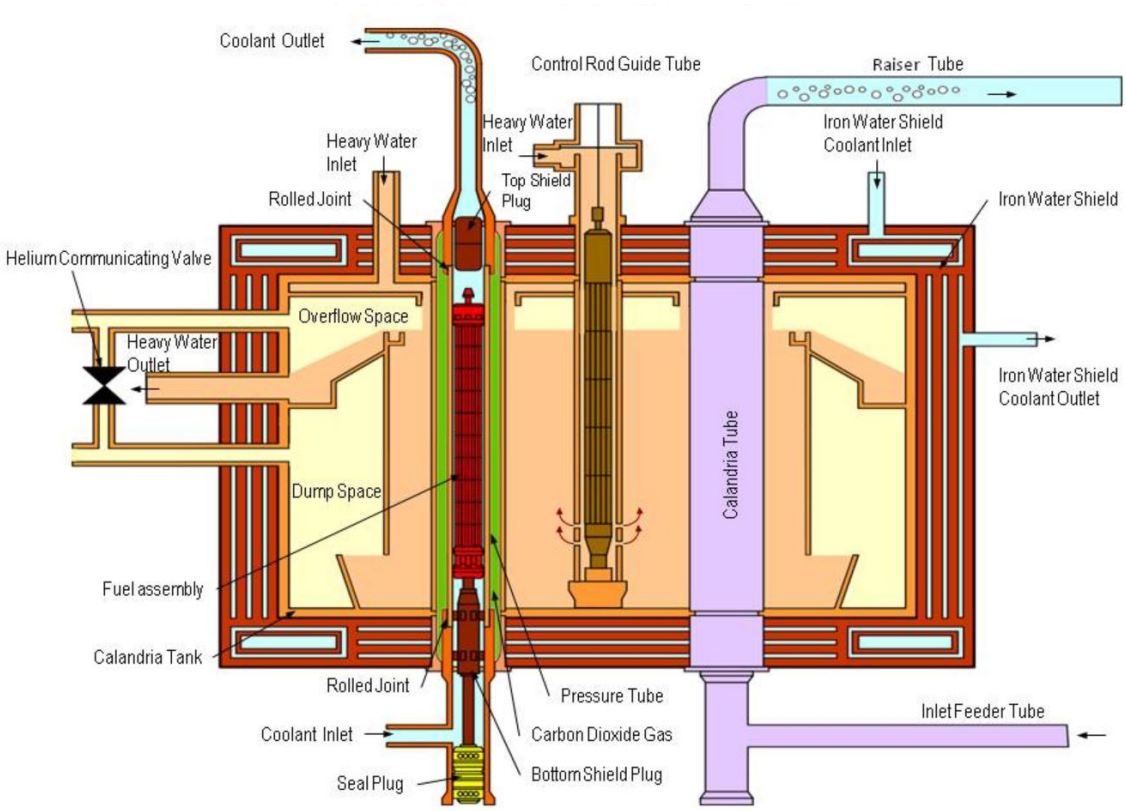

Note. The vertical cross-section of the FUGEN core is shown with indicated directions for the coolant and moderator. From FUGEN Decommissioning Engineering Center (2015, para.11) Copyright 2015 by Fugen Decommissioning Engineering Center. JAEA All Rights Reserved.

Figure 1.4:

Typical FUGEN Core Layout (31st Cycle)

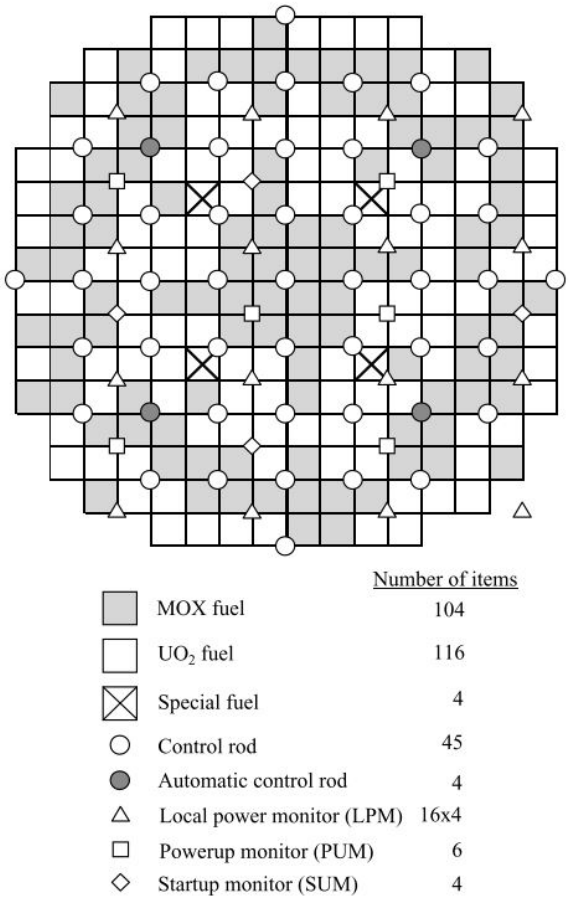

Note. The cross-section of the FUGEN core is shown with indicated locations of different types of fuel as well as control rods locations. From Ohtani et al. (2003, p.962). Copyright 2003 by Taylor and Francis.

The FUGEN reactors refuelling machine was computer-controlled and was located below the main reactor. It was designed for both on and off-load refuelling; however as of 1993, only off-load refuelling techniques had been applied to avoid the risk of pellet-clad interaction, which could occur during on-line refuelling. A schematic of the FUGEN reactor displaying the refuelling machine can be seen in Figure 1.5 (Shiratori, Furubayashi, & Matsumoto, 1993, p.79).

Figure 1.5:

Schematic of Vertical FUGEN Core Showing Refuelling Machine

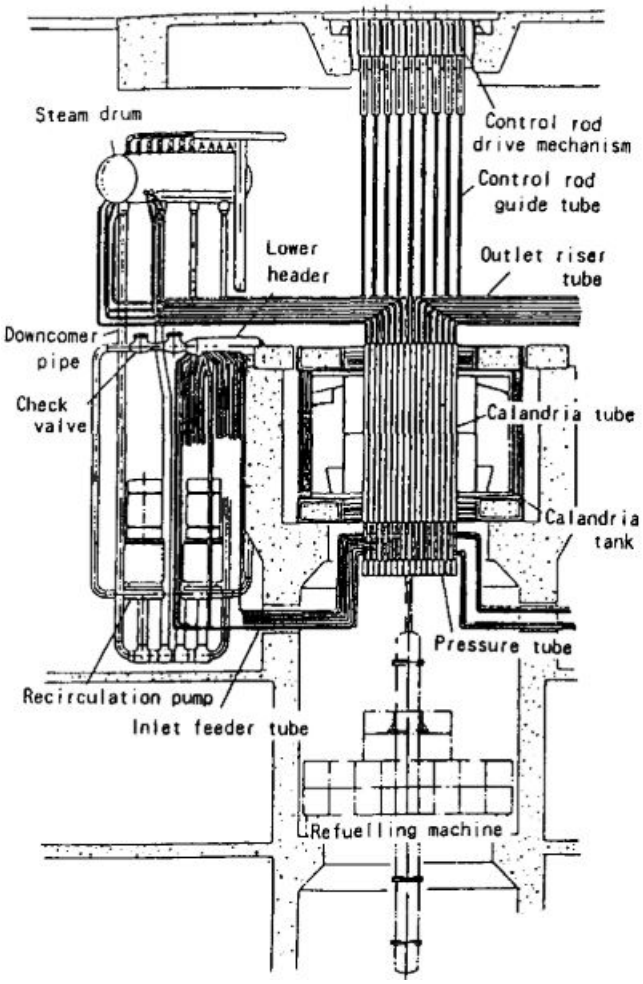

Note. The vertical cross-section of the fugen core is shown indicating the refuelling machine underneath the calandria tank. From Shiratori et al. (1993, p.79). Copyright 1993 by Taylor and Francis.

A computer-aided design (CAD) model of the FUGEN core produced by the Japanese atomic energy agency can help in understanding the different aspects of the vertical cross-section of the FUGEN core. Figure 1.6 below shows the produced CAD model of FUGEN and gives both dimensions of the core, as well as fuel spacing (Tezuka, Koda, Iguchi, Kato, & Yanagihara, 2017, slide.13).

Figure 1.6:

3D CAD Model of FUGEN Nuclear Reactor Core

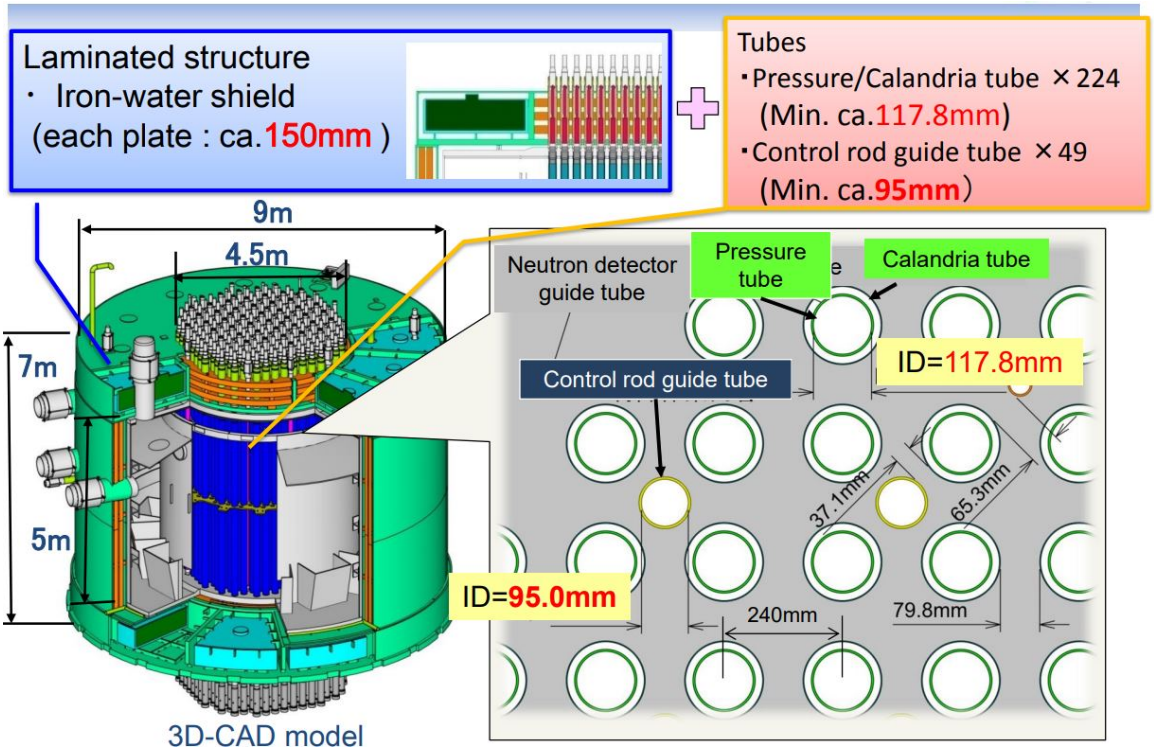

Note. The CAD model shows a 3D representation of the core of the FUGEN reactor showing fuel dimensions. From Tezuka et al. (2017, slide.13). Copyright 2014 by Japan Atomic Energy Agency

1.3 The Pickering Nuclear Reactor of Canada

Throughout this project, a comparison will be made between the FUGEN advanced test reactor (ATR) and a Pickering A reactor. Pickering was operated as two distinct stations with Pickering A containing the first 4 units and Pickering B containing the other 4 units. The first four Pickering Nuclear reactors went into service in 1971. In

1997, these reactors were placed in voluntary lay-up, with units 1 and 4 returning to commercial operation while the others remained in a safe shut-down state. The Pickering reactors being decommissioned were operating for 26 years, one year longer than the FUGEN reactor.

Pickering originally contained 8 Canada Deuterium Uranium (CANDU) reactors that were the first commercial CANDU reactors. The original CANDU reactors in Pickering produced 500 MW each and were the basis for the CANDU-6 reactors, which have become more common around the world (Brooks, 1993). This 500 MW electrical capacity is significantly higher than the 165 MW produced by the FUGEN reactor. The bundle power of a fuel bundle within a CANDU reactor will depend on the number of elements in the bundle. The 28-element bundles found in Pickering have a maximum licensed bundle power of 750 kW, while the 37-element bundles found in Bruce, Darlington, and other CANDU 6 reactors will have a maximum licences bundle power of 935 kW (Rouben, 1999, pg.5). Though realistically, it is expected that the bundles will not constantly be run under their maximum licensed bundle power. The bundle power used in this project is 426 kW which is derived in section 3.4.1.

The reactor design of the Pickering reactor is similar to that of FUGEN. The CANDU reactors are larger and contain horizontal calandria tubes, compared to FUGEN's vertical calandria tubes. They similarly use carbon dioxide as an annulus gas and are heavy-water moderated, allowing for the use of non-enriched fuel. There are some significant differences in the reactor design, however. The first of the differences is that while the FUGEN reactor uses a combination of MOX and slightly enriched UO_2, the CANDU reactor uses unenriched UO_2, called natural uranium dioxide (nUO_2).

A notable difference between reactors is that while both are heavy-water moderated, the FUGEN reactor is light-water cooled. A cross-section of a CANDU fuel channel can be seen in Figure 1.7 (Canadian Nuclear Safety Commission, 2018, slide.6). From Figure 1.7, the use of heavy-water as a coolant as well as carbon dioxide as an annulus gas can be seen.

Figure 1.7:

Cross-Section of CANDU Fuel Channel

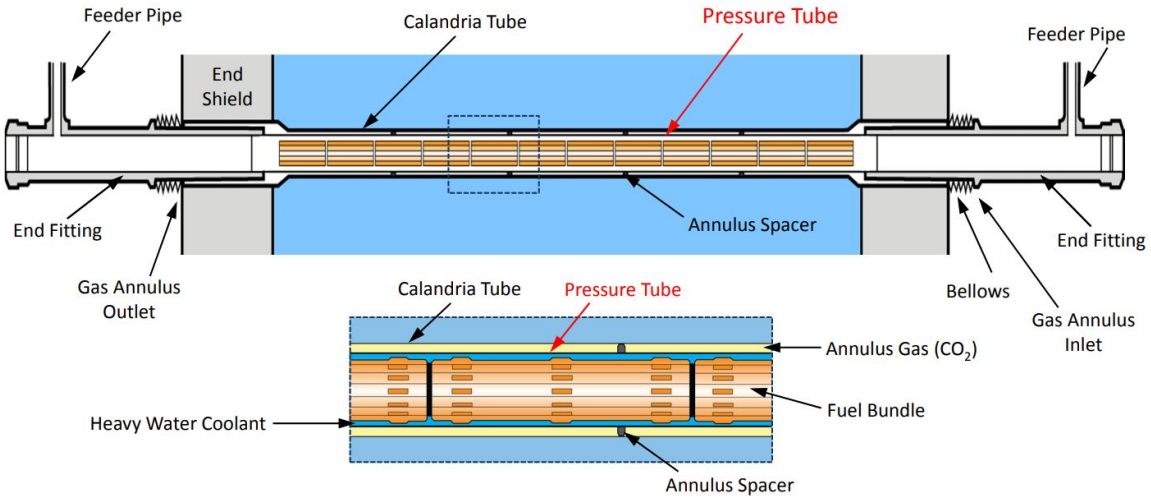

Note. The cross-section of the CANDU reactor shows horizontal calandria tubes and indicates several components of the fuel assembly. From Canadian Nuclear Safety Commission (2018, slide.6). Copyright 2018 by Canadian Nuclear Safety Commission

The CANDU reactor is refuelled using on-line refuelling techniques. This means that as opposed to off-line refuelling, where the reactor is shut-down, and large amounts of the fuel are replaced simultaneously, small amounts of fuel are constantly being replaced throughout the reactor. This on-line refuelling can lead to shorter fuel residency times and lower burnup values, which will subsequently reduce the amount of isotopes produced. Figure 1.8 shows a schematic of a typical CANDU reactor, and includes the location of the refuelling machine within the system (Popov, 2014, pg.15).

Figure 1.8:

Schematic Diagram of a Typical CANDU Heat Transport System

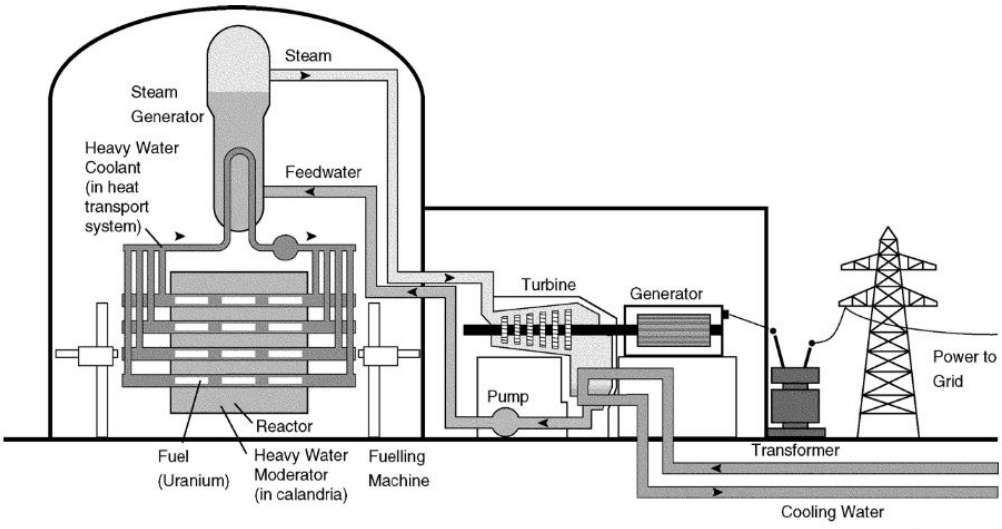

Note. The Figure shows an overview of the entirety of the heat transport system as well as the major components of a CANDU system. From Popov (2014, pg.15). Copyright 2015 by University Network of Excellence in Nuclear Engineering

1.4 Decommissioning of Nuclear Reactors

Once a nuclear reactor has reached the end of its life cycle, its decommissioning phase begins. Decommissioning can be defined as the actions taken in the interest of health, safety, security, and protection of the environment to retire a licensed activity/facility permanently from service and render it to a predetermined end state condition (Harvel, 2019, slide.10). The desired end-state for decommissioning of a nuclear facility may range from site reuse for a new nuclear facility, redevelopment with restrictions on future site use, or site release without restrictions (the green field

state) (Organisation for Economic Co-operation and Development and Nuclear Energy Agency, 2006, pg.17). The amount of radioactive contamination within different areas of a reactor/facility will be key when determining the steps that need to be taken to decommission that reactor/facility.

Contaminated components are typically classified as high, intermediate, or low-level waste. Those components below the given threshold for radioactive contamination, called the clearance level, do not need to be disposed of with the aforementioned levels of waste. When interacting with this waste, standard exemption quantities (EQs) and unconditional clearance levels (UCLs) are specified in schedules 1 and 2, respectively of the nuclear substances and radiation devices regulations (Canadian Nuclear Safety Commission, 2021, pg.34). If the amount of radiation is shown to be below the UCL, the waste can then be treated as nonradioactive, and can be disposed of through normal channels such as being sent off to be recycled.

There are several strategies that can be employed when decommissioning a nuclear reactor/facility. The type of decommissioning strategy used will depend on the amount of time that a site can "cool" before the decommissioning work can begin. Cooling here refers to allowing time for isotopes present to undergo decay and reduce in overall amount within the reactor. This type of decommissioning can entail several strategies such as mothballing, deferred dismantling (safe storage and surveillance), and in-situ entombment (Organisation for Economic Co-operation and Development and Nuclear Energy Agency, 2006, pg.12). These strategies can take decades depending on the amount of radioactivity present and the clearance levels required for decommissioning and can generally be considered passive decommissioning methods.

The other major strategies for decommissioning are used when a site is required to return to its end state in a relatively small amount of time. These techniques involve strategies like prompt decontamination and immediate dismantling (Harvel, 2019). These strategies can be considered active decommissioning methods and require more work than passive methods. Several types of decontamination techniques exist to help lower the activity of isotopes before they can be safe for decommissioning.

Many decontamination techniques can be applied to reduce radioactivity present in an environment. Mechanical and manual decontamination techniques involve using shavers and grinders to remove surface contamination by physically removing the surface contamination of equipment and areas, such as removing the surface of a contaminated concrete wall. Many chemical techniques also exist, from simple cleaners to electro-polishing and ultrasonic decontamination methods. The decontamination factor (DF) is given by:

$$Decontamination\ Factor(DF) = \frac{InitialActivity}{FinalActivity} \tag{1.1}$$

This is the ratio of the initial activity to the final activity of a component and can be used to determine the amount of activity removed. This amount of activity removed is given by:

$$\%\ of\ Activity\ Removed = (1 - \frac{1}{DF}) * 100 \tag{1.2}$$

1.5 Monte Carlo N-Particle Transport Code

The Monte Carlo N-Particle transport code (MCNP) is a general-purpose, continuous energy, generalized geometry, time-dependent coupled neutron/photon/electron Monte Carlo transport code (Girard, Little, White, Lee, & Trellue, 2003). MCNP can be used in several transport modes, including neutron only, photon only, electron only, or any combination thereof. Monte Carlo methods differ from deterministic transport methods, which most commonly solve the transport equation for the average particle behaviour. "Monte Carlo obtains answers by simulating individual particles and recording some aspects (tallies) of their average behaviour" (Girard et al., 2003, pg.2). The average behaviour of particles in the physical system is then inferred from the average behaviour of the simulated particles.

The Monte Carlo method can theoretically duplicate a statistical process such as the interactions between various types of radiations and materials. The individual probabilistic events that comprise a process are simulated sequentially, and the probability distributions governing these events are statistically sampled to describe the total phenomenon. A large number of trials are necessary to describe the desired interaction adequately. The basis of the statistical sampling process is the generation of random numbers (Girard et al., 2003). The Monte Carlo methods follow individual particles throughout their entire path from their source to their end. As many of these neutron/photon paths are tracked, neutron and photon distributions become better known and user-defined quantities of interest are tallied. The more tracked paths, the more accurate the results will be.

1.6 MCNP Depletion Code

Generally, Monte Carlo depletion codes can be divided into two categories based on their cross-section creation methodology. The first type of code uses one-group reaction rates, which are tallied for all cross-sections of interest directly by the Monte Carlo code. The second type uses a multi-group approach for cross-section generation. In this method only the multi-group flux is calculated in this method while reaction rates for particular nuclides are not tallied. Reaction rates are then calculated separately using pre-generated multi-group cross-sections and the fine group neutron spectrum obtained from the Monte Carlo code (Bomboni, Cerullo, Fridman, Lomonaco, & Shwageraus, 2010). MCNP utilizes the second approach, which reduces the code execution time without affecting its accuracy.

MCNP6 performs depletion calculations via the integration of the CINDER90 library. MCNP6 runs a steady-state calculation to determine the system eigenvalue, 63-group fluxes, energy-integrated reaction rates, fission multiplicity and recoverable energy per fission (Q values). CINDER90 then takes those MCNP6-generated values and performs the depletion calculation to generate new atom densities for the next time step. MCNP6 takes these new atom densities and generates another set of fluxes and reaction rates. The process repeats itself until after the final time step specified by the user (Werner et al., 2017). The standard depletion equation (Fensin, James, Hendricks, & Goorley, 2011, pg.2) used by CINDER90 is given by:

$$\frac{dN_m(t)}{dt} = -N_m(t)\beta_m + \bar{Y}_m + \sum_{k \neq m} N_k(t)\gamma_{k \to m} \tag{1.3}$$

where $N_m(t)$ is the time dependent isotope density of nuclide m, β_m is the destruction coefficient for nuclide m, $\gamma_{k\to m}$ is the creation coefficient for nuclide m from nuclide k, $\bar{Y}_m$ is the feed or removal rate, and $N_k(t)$ is the time dependent isotope density of nuclide k.

An example of the CINDER90 library for ^{235}U(n,f) can be seen in Figure 1.9 (Micklich, 2015, slide.8). CINDER will use these libraries and the depletion equation above, which gives the atom density at each step to propagate the creation of new isotopes throughout the fission process.

Figure 1.9:

CINDER Data Libraries $^{235}U(n,f)$ Cross Section

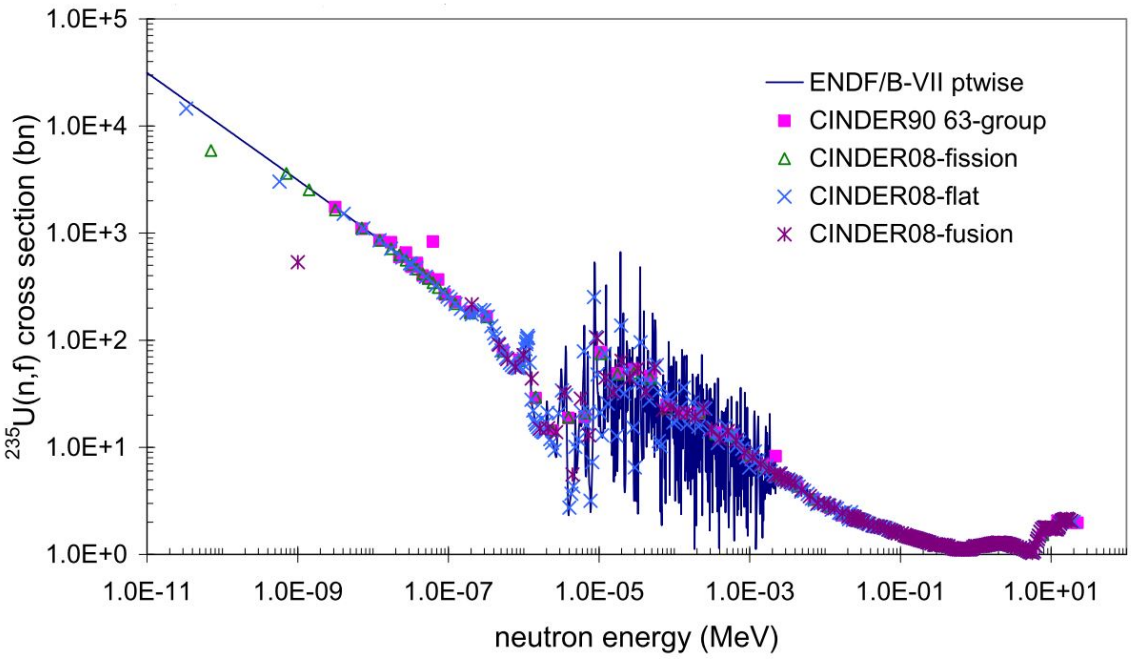

Note. The Figure shows an example of a neutron-fission cross-section, specifically the ^{235}U(n,f) cross-section. When a neutron with an energy in this range interacts with ^{235}U it is likely to induce a fission reaction. From Micklich (2015, slide.8). Copyright 2015 by Argonne National Laboratory.

1.7 The MCNP Input File

All MCNP input files start with the same basic structure and building blocks. This basic structure consists of code blocks, called "cards" within MCNP, that must be placed in a specific order. This naming convention comes from using punch cards as inputs into old computer systems. An MCNP input file can be broken into three major chunks, the cell cards, the surface cards, and the data cards. A particular benefit to the newest versions of MCNP is an allowance for the input file to be 128 columns wide. This column width allows for easier in-line commenting and helps in reducing the length of input files in general.

The cell cards are where the contents of cells are specified. Cells in MCNP are surface geometry specifications used to describe regions within the model. Within these cells, their relative orientation with regard to each other is specified. An example of this is specifying a region within six planes as the inside of a cube, or the region outside of these surfaces as a void where particle transport equations are not completed. Some properties of the cells are also defined in the cell cards, such as the density and type of material which encompasses the region defined by the cell geometries.

In the surface cards, the bounds and shapes of the cells are described. This can either be done by applying a combination of several surface equations or more simply through the use of macrobodies. Take, for example, the creation of the cube previously described. Using traditional surface equations, it takes six planes to define this cube. However, this can make the boolean values required to define cells in MCNP complex due to the large number of surfaces. Macrobodies allow MCNP to create a singular surface by choosing the location of a corner of the box and describing the three

perpendicular vectors that allow for its creation. These macrobodies make the boolean determinations required in the cell card easier. Rather than defining the cell within the box using the boolean values of 6 surfaces, the cell can be described as simply being within the one bounding surface of the macrobody.

The final cards required for the input file in MCNP are the data cards. The data cards contain several vital pieces of information, such as the material specifications, the source definition, the tally declarations and more. It is within these cards that MCNP is told to complete an action, such as performing depletion calculations. Examples of the programming of the MCNP input file can be found in section 3.6 as well as in Appendix A and B.

1.8 Defining a Source in MCNP

The data and burn cards must be defined to determine the isotopic inventory in the reactors. For MCNP to begin running calculations using the designed models, it is necessary to designate the radiation source. There are three primary methods of defining a starting particle in MCNP simulations concerning criticality calculations.

The KCODE card specifies in MCNP6 that a criticality source will be used in determining k_{eff}. The criticality source uses total fission values and applies only to neutron problems. Fission sites for each cycle are those points generated in the previous cycle. For the initial cycle, fission sites can come from an SRCTP file from a similar geometry, a KSRC card, or a volume distribution specified by an SDEF card (Werner et al., 2017).

In the KCODE card, MCNP automatically generates fission source points in the fuel based on the material specifications of the fuel as well as the starting points defined in the KSRC card. In the early runs of the model, the criticality source grows to encompass the entirety of the fuel, and based on (n,f) interactions, a complex set of nuclides is generated using the inbuilt actinide nuclear data libraries (Fensin et al., 2011). The KCODE keeps track of the generated isotopes and if any of these generated isotopes are made of fissionable material, then they are included as part of the criticality source in the next cycle.

The KCODE card is different from the other source specifications in that the user only needs to create a reasonable representation of the fissionable areas, and the KCODE will automatically generate a complex criticality source from the specified initial source points. It does this by propagating the criticality source throughout the fuel until the entirety of the fissionable materials in the model are encompassed. Based on the complexity of the model, a greater number of the early runs may need to be discarded to give time for the criticality source to fully represent the modelled fuel. Compared to an SDEF card in which the source must be defined by its starting cell, position, starting energy, starting weight, and the source particle type, the use of the KCODE card is simpler to input into MCNP as all that is required to use a KCODE card are the geometry descriptions and the material specifications of the model. Due to the automatic use of the inbuilt actinide nuclear libraries, the generated criticality source is more complex than the SDEF as it will account for the wide array of neutrons and nuclides generated from the fissioning of fuel.

The simplest way to set the starting source point is to use a criticality source point using the KSRC card. This card contains triplets, which are the coordinates of the initial source points for a KCODE calculation. The KSRC card is the most forgiving source definition as it is unnecessary to input all of the coordinate points. The only

thing required for the KSRC card is that at least one point must be specified within a cell containing fissile material, and this point must be away from cell boundaries. Usually, one source point in each fissile material region is adequate as MCNP will quickly calculate and use the new fission source distribution. SDEF cards can be used to set up tallies using the isotopic composition of the spent fuel at the end of the burnup calculations.

1.9 Literature Review

Over the years, the interest in the decommissioning of reactors has grown as the current fleet of reactors ages. Many studies have worked on modelling reactors for the sake of decommissioning by simulating fuel burnup and isotope production. MCNP has been used for decades to predict the isotopic content of radionuclides within components of interest. This literature review focuses on the use of tools such as MCNP to predict the isotopic content of reactors for the purposes of decommissioning and how MCNP's capabilities have developed over the years. There are many methods of performing burnup calculations, from rough hand calculations to the use of a well set up excel file. It is both the popularity of MCNP as well as the inbuilt MCNP data libraries that cause MCNP to be the program of choice when performing the burnup calculations.

Early use of MCNP's capabilities for the purpose of decommissioning was used by the Idaho national labs in order to perform an activation analysis in order to characterize the activated metals from reactor decommissioning waste. This analysis used MCNP's neutron activation capabilities and did not entail the use of burnup calculations. However, this research ran into computational issues due to the size of the model

and modelling approximations. This is an expected issue for the time due to the computational limitations of 1995. Uncertainties within the material compositions of the model were also of concern as there was a lack of information on the presence of ^{93}Nb and ^{94}Mo within the base metals (Love, Pauley, & Reid, 1995).

Interest began to grow in MCNP based depletion codes with the growing computer capabilities. In the past, the MCNP transport code was commonly paired with an external depletion code, such as ORIGEN2. Examples of these programs include BURNPRO, BGCORE, and MONTEBURNS (Bomboni et al., 2010). Programs like MONTEBURNS were created in order to automatically perform depletion calculations where MCNP provided one-group microscopic cross-sections and fluxes to the chosen depletion code of either ORIGEN2 or CINDER90 (Trellue, Poston, & User's Manual, 1999). As time went on, a self-contained Monte-Carlo linked depletion capability became increasingly desirable. In his PhD thesis, Michael L. Fensin studied the integration of the CINDER90 library into MCNPX. His research showed how all linked depletion methodologies suffer from how the linking process affects the functionality of both codes and how the self-contained depletion capabilities of MCNPX would solve this. Some of the limitations no longer faced were how MONTEBURNS was not capable of following multiple isotope transmutations at multiple temperatures (Fensin, 2008).

Several decommissioning studies have been performed using MCNP to determine the radionuclide inventories of reactors. A study was performed by the Korean Atomic Energy Research Institute in which the concentration of ^{94}Nb in a CANDU reactor was estimated at several locations in the reactor using a combination of MCNP and ORIGEN2 and compared with the measured nuclide inventory. This research found that the MCNP/ORIGEN2 system and source term characterization method proposed was a viable option to estimate the source terms of the decommissioning waste from a

CANDU reactor (Cho, Sun, Choi, Yang, & Hwang, 2011). This statement, however, should be taken cautiously as the study found that the measured data was only within a range of 30% of the MCNP model. Despite this 30% difference range, the study found that this was similar enough to provide high confidence in the calculation method.

The studies discussed in this literature review show that MCNP has been used several times in research when estimating the isotopic inventory of nuclear reactors, and has been used to calculate neutron activation for several decades. Recent additions to the MCNP code have allowed for MCNP to perform burnup calculations accurately while not relying on the use of other codes such as ORIGEN2. The lack of information on material concentrations in the metals of the reactor continues to be an issue, as estimates and assumptions must still be used.

1.10 Thesis Outline

The purpose of this thesis is to find the reason as to why the chosen isotopes are of interest to either Canada or Japan. The background section has given a background on the necessary information for the Pickering and FUGEN reactors, as well as on MCNP and its use as a tool to perform burnup calculations on nuclear fuel.

The second chapter focuses on the production of isotopes within a reactor. In this chapter, neutron interactions and how they lead to the creation of activation and fission products is discussed. This chapter then discusses the Canadian law on unconditional clearance limits and exemption quantities. The chapter ends with the identification and radiological hazards of the isotopes of interest to this project.

The third chapter focuses on the methodology of the research. It begins with a section on the use of fuel burnup as a gauge of isotope production within the MCNP models. The chapter then focusses on the fuel parameters and dimensional data that will go into the creation of the Pickering and FUGEN models. After this the geometries of the MCNP models are compared with reference schematics and differences are discussed. The chapter ends with a section on the specifics of modelling the data discussed earlier in the chapter into an MCNP input file.

The fourth chapter focuses on the results of using the MCNP models and how these values and the normalization of the data allow for the direct comparison of the Pickering and FUGEN models. The discussion section focuses on the meaning of the attained results and discusses how they relate to each other as well as how they relate to real-world comparisons.

The fifth chapter focuses on the conclusions of the research and answers the questions posed in the thesis' problem statement. It then discusses future work that can be done in the field and areas where the research could be improved.

Chapter 2

How Radioactive Isotopes are formed in a Reactor and the Associated Radiological Hazards

2.1 Neutron Interactions

There are many forms of radiation interaction; however, those most relevant to isotope production in a reactor will be neutron interactions. Like gamma rays, neutrons carry no charge and therefore cannot interact in matter through the Coulomb force, more simply described as the repulsion and attraction of charged particles. This is an important distinction as the coulomb force largely "governs the energy loss mechanisms for charged particles and electrons" (Knoll, 2010, pg.53). When neutrons undergo interactions, it is always with the nucleus of the absorbing material. As a result of

this interaction, the neutron may either totally disappear, be replaced by secondary radiation, or undergo a significant change in direction. Unlike gamma rays, however, "the secondary radiations formed from neutron interactions are almost always heavy charged particles" (Knoll, 2010, pg.53).

The most significant interactions for slow neutrons include both elastic scattering interactions with absorber nuclei as well as a large set of neutron-induced nuclear reactions. These elastic collisions tend to be highly probable and will often bring the slow neutron into thermal equilibrium with the absorber medium before a different type of interaction can occur. Much of the population in the slow neutron energy range will therefore be found among these thermal neutrons, which at room temperature have an average energy of about 0.025 eV (Knoll, 2010, pg.54). This range for (n,fission) interactions, in which a neutron causes fissioning in the absorber medium, can be seen in Figure 2.1 for ^{235}U and ^{239}Pu (Kerlin & Upadhyaya, 2019, pg.76). The most common slow neutron interaction will be the radiative capture reaction (n,γ), in which a gamma-ray will be created as a secondary radiation. This interaction plays an important part in the attenuation and shielding of neutrons.

While the probability of neutron interactions significantly decreases with increasing neutron energy, the importance of scattering also increases. This is because of the large amount of energy that can be transferred in one collision. These collisions produce recoil nuclei as secondary radiation which will have gained a detectable amount of energy (Knoll, 2010). The most efficient neutron moderation occurs when the scattering nuclei are sized similarly to the incident neutron, as the interaction can cause the neutron to lose almost all of its energy. Due to the similar size between neutrons and hydrogen atoms, hydrogenous materials, most commonly water, are used for neutron moderation, as the large amount of hydrogen atoms will effectively slow the neutrons into the slow region described previously.

Figure 2.1:

Neutron Cross-Sections for Fission of Uranium and Plutonium

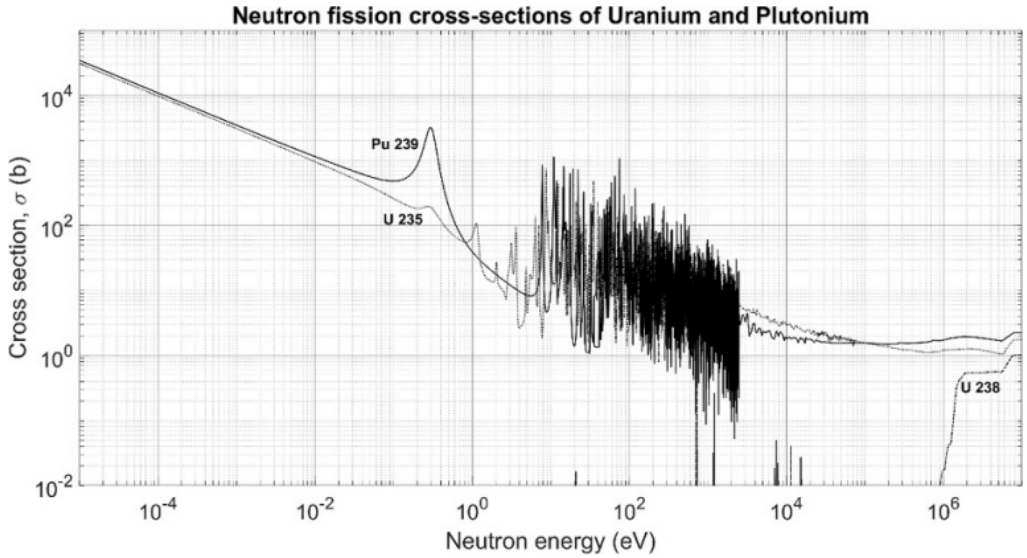

Note. The Figure shows the neutron energy rnge for uranium and plutonium where fission is likely. From Kerlin and Upadhyaya (2019, pg.76). Copyright 2019 by Elsevier Inc.

2.2 Fission Products

The primary method of radionuclide production in a nuclear reactor is fissioning fuel. FUGEN uses a uranium-plutonium mixed oxide (MOX) fuel. As a result, the primary fissile content of the FUGEN reactor consists of ^{235}U, ^{239}Pu, and ^{241}Pu (Tanaka, Maeda, Sasaki, Ikusawa, & Abe, 2006, pg.59). The fissioning of these elements will create several nuclides, the analysis of which will allow for a comparison of the fuel assemblies of both reactors. The Pickering reactor, which utilizes natural UO_2 however, will primarily fission ^{235}U, and as such, will have a more limited variety of fission products compared to the MOX fission. This is because even though natural UO_2 generates plutonium through neutron activation, the amount created is extremely

small when compared to MOX fuel which originally contains plutonium. When nuclei undergo fission, they can undergo either symmetric or asymmetric fission. Symmetric fission, or the fissioning of a parent isotope into two equal nuclides, is not the preferred outcome of fission reactions. Asymmetric fission is much more preferred, as can be seen in Figure 2.2 showing three sets of fission yield peaks for ^{233}U, ^{239}Pu and ^{235}U. If symmetric fission were the preferred outcome, then Figure 2.2 would appear as a single peak centred approximately at a mass number of 115. This bias for asymmetric fission is due to the presence of magic numbers. Fission reactions prefer to form at least one product with a magic number of protons or neutrons because of the stability of those nuclides (Bryan, 2018). The magic number used here is defined as the number of protons and neutrons required to form stable shells within the atomic nucleus.

Figure 2.2:

Fission Yield for ^{233}U, ^{239}Pu *and* ^{235}U

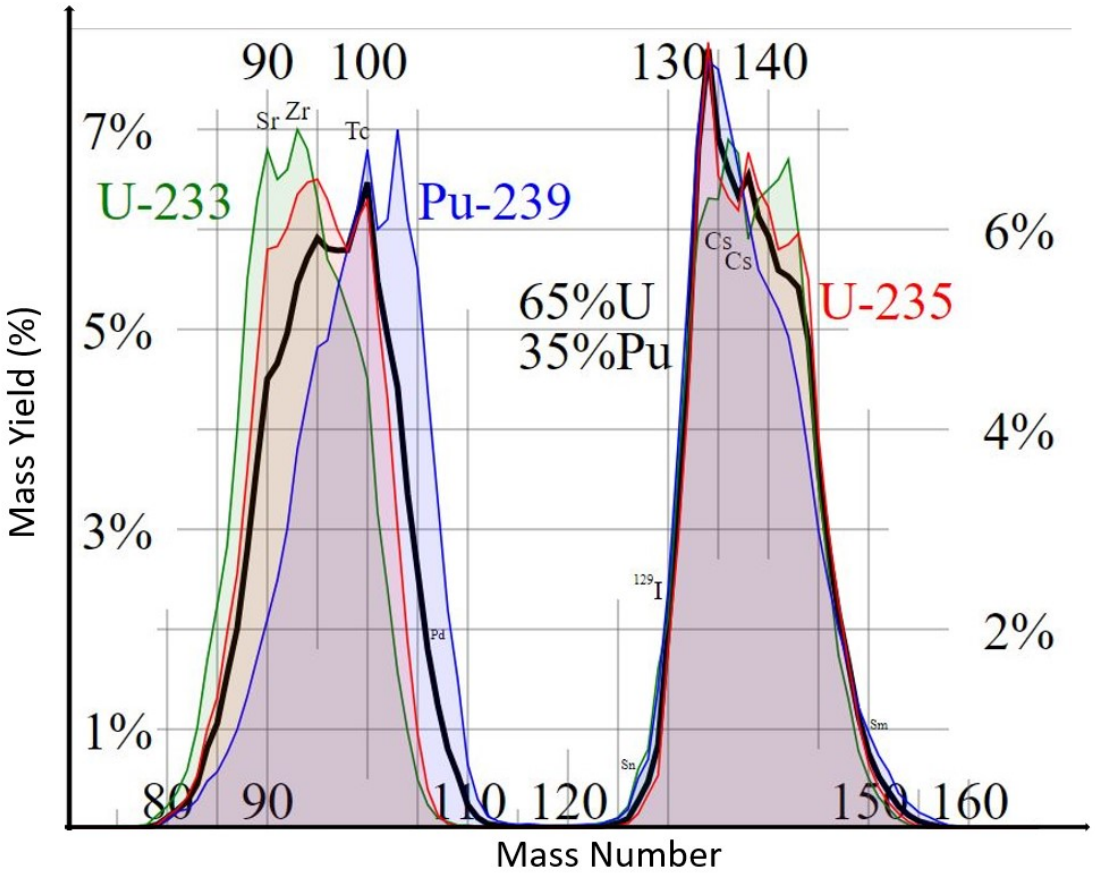

Note. The Figure shows the percent yields from the fissioning of four different major fuel elements. ^{233}U is represented in green, ^{235}U is represented in red, ^{239}Pu is represented in blue, and a combination of 65% U and 35% Pu is represented in black. Adapted from *Fission product yield* (2008) Copyright 2008 available from creative commons

2.3 Neutron Activation

The other method of radioisotope production within a reactor is neutron activation. Neutron activation is the production of a radionuclide by absorption of a neutron. This reaction can come in many forms such as (n, γ), (n, α), (n, β) or (n, p). If a radionuclide is being created by neutron irradiation and is decaying simultaneously, the net number of radioactive atoms present in the sample at any time is the difference between the rate of production and the rate of decay. This may be expressed mathematically by:

$$\lambda N = \phi \sigma n (1 - e^{-\lambda t}) \tag{2.1}$$

where ϕ is the flux $(neutrons/cm^2/s)$, σ is the activation cross section (cm^2), λ is the $\frac{0.693}{T_{1/2}}$ is the transformation constant of the induced activity, $T_{1/2}$ is the half-life, N is the number of radioactive atoms, and n is the number of target atoms (assumed to be constant during irradiation. The term $\phi \sigma n$ is sometimes called the saturation activity. For an infinitely long irradiation time, it represents the maximum obtainable activity with any given neutron flux (Cember & Johnson, 2008, pg.193).

For many materials, absorption of a neutron produces a radionuclide with a half-life ranging from a fraction of a second to many years. The radiation produced by the subsequent decay of these activation nuclei may be very significant for materials that have been exposed to large neutron fluences, especially structural components in a reactor core (Shultis & Faw, 2000).

2.4 Leakage of Isotopes from the Fuel

In an ideal reactor, the fission products will stay within the fuel sheath and be entirely removed when the fuel is taken out of the reactor. For the sake of computer simulations of reactors, this will most often be the case. However, damage to core elements and leakage into the calandria is not unexpected in real-world situations. Over the several decades that reactors run, components will experience corrosion and material degradation, fittings will leak, and relatively small amounts of isotopes will be released outside the fuel and remain within the reactor. These isotopes can build up over time and cause issues when it comes time to decommission the reactor finally. For example, ^{137}Cs is a fission product of ^{135}U and can cause issues when decommissioning due to its hard gammas and its 30 year long half-life, which means it could take several hundred years for any contaminated materials to decrease below clearance levels as materials contaminated with ^{137}Cs are known to remain radioactive for centuries. For example, if a material has a reactivity concentration of 1 Bq/g of ^{137}Cs, it would take approximately 100 years before it reached the clearance level for ^{137}Cs of 0.1 Bq/g (Department of Justice Canada, 2000, pg.46). This is given by:

$$A = A_0(0.5)^{\frac{t}{T_{1/2}}} \tag{2.2}$$

where A is the current activity of the component, A_0 is the original activity of the component and $T_{1/2}$ is the half-life of the ^{137}Cs of 30.17 years. Inputting these values into equation 2.2 gives a time of 100.2 years

$$0.1\frac{Bq}{g} = 1\frac{Bq}{g}(0.5)^{\frac{t}{30.17yr}} \rightarrow t = 100.2 years$$

2.5 Unconditional Clearance Limits

Once a piece of radiologically contaminated equipment is determined to be below clearance levels, it is released from regulator control and can be disposed of as desired. "The primary radiological basis for the exemption of bulk amounts of material for radioactive clearance is that the effective doses to individuals should be of the order of 10 µSv or less in a year" (*Application of the Concepts of Exclusion, Exemption and Clearance*, 2004, pg.9). The measure for the radioactivity of a material is its activity concentration, often given in units of Bq/g or Bq/cm^3. In the case of objects large enough to self-shield their emitted radiation, a surface activity measurement is taken in units of Bq/cm^2. The non-metric unit for radioactivity, which will often be seen in this thesis, is the curie (Ci). The curie is based on the decay of ^{226}Ra and can be defined mathematically as 1 Ci equalling 37 GBq. Both Canada and Japan follow the IAEA guides strictly. When reading through their respective regulatory documents, it can be seen that the clearance levels for both countries are compliant with SAFETY GUIDE No. RS-G-1.7. The use of SAFETY GUIDE No. RS-G-1.7 in the regulation of each country can be seen in (Hattori, 2020, pg.103) for Japan and (Department of Justice Canada, 2000, pg.1) for Canada. The clearance level of a material is decided on a per radionuclide basis. Radionuclides which are more hazardous, such as those with hard energy gamma-ray emissions, will only be exempted given a much lower activity than relatively harmless nuclides, such as α emitters.

The government of Canada describes exemption quantities for each radioactive nuclide listed in column 1 of Schedule 1 of section 44 of the Canadian nuclear safety and control act, Nuclear Substances and Radiation Devices Regulations (Department of Justice Canada, 2000, pg.33). The values listed in this section are the exemption quantities for radionuclides which is the deciding factor for determining whether a material which does not currently have a license should be licensed. Column 1 of

schedule 2 of the regulations pertains to the limits for unconditional clearance, under which a licensed material can be removed from its license (Department of Justice Canada, 2000, pg.45). Any materials with activity concentrations found to be below the unconditional clearance limit do not need to be regarded as radioactive waste. For those isotopes not in column 1 of Schedule 2, if the atomic number of the substance is less than or equal to 81, its unconditional clearance limit is 1 Bq/g. If the atomic number of the substance is greater than 81 and the substance or its short-lived progeny do not emit alpha radiation, then its unconditional clearance limit is 1 Bq/g. If the atomic number of the substance is greater than 81 and the substance does emit alpha radiation, then its unconditional clearance limit is 0.1 Bq/g (Department of Justice Canada, 2000, pg.5).

2.6 Radiological and Biological Hazards Associated with the Isotopes of Interest

The isotopes described in this project are important when decommissioning nuclear reactors/facilities due to the potential harm they present to the people doing the decommissioning work. This section discusses the radiological and biological hazards associated with the special isotopes central to this project. This potential harm comes from the radioactive decay of these isotopes. As discussed previously, as they decay, these isotopes will emit either photons or heavy charged particles, which can cause bodily harm when absorbed into organs or tissue. Table 2.1 below shows the thresholds for radiations damage to several types of tissues and organs (Cember & Johnson, 2008, pg.282). Without prior knowledge about the presence and location of these radioactive isotopes, it is possible for those working on these reactors to receive unexpected doses, which can lead to any of the effects listed in Table 2.1.

Table 2.1:

Estimates for the Thresholds for Significant Detrimental Deterministic Effects

ORGAN	INJURY AT 5 YRS	1–5% DOSE (Gy)	25–50% DOSE (Gy)
Liver	Failure	35	45
Kidney	Nephrosclerosis	23	28
Bladder	Ulcer	60	80
Testes	Permanent sterilization	5–15	20
Ovaries	Permanent sterilization	2–3	6–12
Thyroid	Hypothyroidism	45	150
Breast	Atrophy	<50	<100

Note. The Table shows the doses in Gy that will cause injury at 5 years to a % of the affected population. From Cember and Johnson (2008, pg.282). Copyright 2009 by The McGraw-Hill Companies

The radiological and biological hazards associated with these isotopes largely determine whether they are of interest to decommissioning. Each isotope affects the workers and environment uniquely, which must be discussed before decommissioning the reactor.

^{93}Mo

Molybdenum is a transition metal and is an essential element for plants, animals, and humans, present in two groups of enzymes: the nitrogenases and the molybdopterins. Little information is available on the behaviour of inhaled molybdenum in humans following accidental intakes or from experimental studies in animals. The clearance of molybdenum is rapid, with the mean transit time in plasma calculated to be approximately 150 min. Urinary excretion in the first day after intake ranged between 30% and 80% of the intake, with most of the intake being excreted within 8-12 h

(Paquet et al., 2016). ^{93}Mo has a half-life of 4000 years and decays primarily through electron capture. The decay of ^{93}Mo emits an electron with an energy of 0.0056 MeV per nuclear transition and a photon that has an energy of 0.0107 MeV per nuclear transition (Eckerman & Endo, 2008).

^{108m}Ag

In general, inhaled silver shows minimal (less than l %) urinary excretion in mammals, is about 90 % excreted during the first 30 d and has an initial biological half-life in the lung in the order of a few days or less. The organ receiving the highest dose per unit of activity inhaled will depend on the physical half-life of the particular isotope. For example, a relatively short-lived isotope like ^{106}Ag (half-life = 8.5 d) may irradiate the lung most heavily, while ^{110m}Ag (half-life = 255 d) may irradiate the liver more (Phalen, Morrow, Raabe, & Velasquez, 1973). ^{108m}Ag has a half-life of 418 years and as such is expected to more heavily irradiate the liver. ^{108m}Ag decays primarily through electron capture and isomeric transition. The decay of ^{108m}Ag emits an electron with an energy of 0.0159 MeV per nuclear transition and a photon with an energy of 1.6209 MeV per nuclear transition (Eckerman & Endo, 2008).

^{134}Cs

Caesium is an alkali metal that only occurs in oxidation state I. Caesium may be encountered in various industries in a variety of chemical and physical forms, including soluble inorganic salts (chloride, nitrate) and less soluble sulphates (International Commission on Radiological Protection, 2017, pg.137). “Since radioactive caesium has similar chemical properties to potassium, it will be distributed throughout the body, like potassium” (Ministry of the Environment, Government of Japan, 2018,

pg.31). The biological and effective half-life of caesium inside the body of an adult is approximately 110 d (Agency for Toxic Substances and Disease Registry (ATSDR), 2004, pg.162). ^{134}Cs has a half-life of 2.06 years and decays via either electron capture or through a beta negative decay. The decay of ^{134}Cs emits an electron with an energy of 0.1639 MeV per nuclear transition and a photon with an energy of 1.5551 MeV per nuclear transition (Eckerman & Endo, 2008).

^{166m}Ho

Holmium is an element of the lanthanide series and may be encountered in various chemical and physical forms. Holmium is most commonly obtained from gadolinite and monazite. Biokinetics for holmium can be estimated based on studies performed on rats. From the intake activity, approximately 60% of the holmium was found to be deposited in the skeleton. 10% was deposited in the liver. By day four, the cumulative loss in the urine amount to approximately 15-28 % of the amount reaching the blood (Paquet et al., 2019). ^{166m}Ho has a half-life of 1200 years and decays via beta negative decay. The decay of ^{166m}Ho emits an electron with an energy of 0.1497 MeV per nuclear transition and a photon with an energy of 1.6249 MeV per nuclear transition (Eckerman & Endo, 2008).

^{243}Am

Americium is an actinide element that may be encountered in industrial use in a variety of chemical and physical forms. The most commonly found isotopes of americium found in nuclear reactors are ^{240}Am, and ^{241}Am. There is a large amount of information available on the behaviour of americium's biokinetics. Studies have found that all compounds of americium have been shown to absorb into the blood with half-times

of several tens of days. Autopsies on patients exposed to ^{241}Am have shown the systematic burden of the skeleton, liver, kidneys, and other soft tissues to be 82.3%, 6.4%, 0.25%, and 11.0% respectively (Paquet et al., 2019). ^{243}Am has a half-life of 7370 years and decays via alpha decay. The decay of ^{243}Am emits an alpha particle with the energy of 5.3583 MeV per nuclear transition, an electron with an energy of 0.0234 MeV per nuclear transition, and a photon with an energy of 0.0585 Mev per nuclear transition (Eckerman & Endo, 2008).

^{121m}Sn

Several animal trials have been performed to understand the biokinetics of radioactive tin. Injections of ^{113}Sn into lab rats have shown excretion of 35% of the original intake in the urine and 12% in the feces. In bile-duct cannulated rats, 23% was excreted in the urine, 11% in bile, and 2% in the feces. These observations indicate that urine and bile appear to be significant routes of excretion of absorbed tin (Agency for Toxic Substances and Disease Registry (ATSDR), 2005). ^{121m}Sn has a half-life of 43.9 years and decays through isomeric transition and beta negative decay. The decay of ^{121m}Sn emits both an electron that has an energy of 0.0354 MeV per nuclear transition and a photon with an energy of 0.0052 MeV per nuclear transition (Eckerman & Endo, 2008).

^{41}Ca

Calcium is an alkaline earth element that is an essential element of life. Common isotopes found in medicine are ^{45}Ca and ^{47}Ca. Calcium has a removal half-time of 100 d and is considered to be lost from the body by urinary or fecal excretion only. It is estimated that 58% of the calcium leaving blood moves to the rapid-turnover

soft tissue while 25% is transferred to the bone surface compartments (Paquet et al., 2016). ^{41}Ca has a half-life of 10200 years and decays through electron capture. The decay of ^{41}Ca emits an electron with an energy of 0.0027 MeV per nuclear transition and a photon with an energy of 0.0005 MeV per nuclear transition (Eckerman & Endo, 2008).

2.7 Isotopes of Interest

There are various reasons why an isotope would be of interest to decommissioning a nuclear reactor. These reasons can be radiological, biological, or chemical, as discussed previously. This project will make the assumption that the reasons as to why they are of interest are radiological, and focus on the radiological reasons as to why an isotope is considered of interest. An extensive list of the isotopes of interest to the decommissioning of reactors within Canada and Japan can be seen in Table 2.2. Throughout this project, these chosen isotopes of interest, referred to as the special isotopes, are special due to the fact that they are not considered to be of interest to both countries regulatory bodies. It is the goal of this research to explain why they are of interest to one nation and not the other by comparing the inventory produced within the fuel of reactors from each country.

Table 2.2:

Radionuclides of Interest to Canada and Japan for Decommissioning

Radionuclide	Canada	Japan	Half-life(year)
C-14	Yes	Yes	5568
Fe-55	Yes	Yes	3
Ni-59	Yes	No	75000
Co-60	Yes	Yes	5
Ni-63	Yes	Yes	96
Zr-93	Yes	Yes	78
Nb-94	Yes	Yes	20300
H-3	Yes	Yes	12
Cl-36	Yes	Yes	308000
Ca-41	Yes	No	99000
Sr-90	Yes	Yes	29
Nb-93m	Yes	No	14
Tc-99	Yes	Yes	210000
Sn-121m	Yes	No	55
Sb-125	Yes	Yes	3
Te-125m	Yes	No	0.15
I-129	Yes	No	16000000
Cs-137	Yes	Yes	30
Eu-152	Yes	No	14
Eu-154	Yes	Yes	9
Pu-238	Yes	Yes	88
Pu-239	Yes	Yes	24000
Pu-240	Yes	Yes	6561
Pu-241	Yes	No	12
Am-241	Yes	Yes	432
Cm-244	Yes	Yes	18
Mo-93	No	Yes	4000
Ag-108m	No	Yes	418
Cs-134	No	Yes	2
Ho-166m	No	Yes	1200
Am-243	No	Yes	7370

Note. The Table shows whether the specified radionuclides are of interest to the decommissioning of reactors/facilities in Canada or Japan and indicates the half-lives of these nuclide. (G. Harvel, personal communication, August 4, 2021).

Several factors can affect whether an isotope is considered to be of interest. One of the major factors that make an isotope be of interest is its half-life. If it has a very short half-life, it may not be considered of interest as it could decay away and no longer be considered harmful. An example of this within the isotopes specified for this project is the relatively short half-life of ^{134}Cs of only two years. Another factor affecting whether an isotope is of interest is its abundance. At a minimum, only isotopes with a radioactive concentration high enough to be above the exemption levels will be considered to be of interest. A third factor affecting why an isotope is of interest is its location in the reactor. It is crucial when decommissioning a reactor to know the specific risks associated with each part, which becomes difficult due to neutron activation or leaks within the fuel.

Of particular interest to this project are the discrepancies between the two countries. The radionuclide which Canada considers to be of interest which Japan do not are ^{59}Ni, ^{41}Ca, ^{93m}Nb, ^{121m}Sn, ^{125m}Te, ^{129}I, ^{152}Eu, and ^{241}Pu. The radionuclides which are of a concern to Japan and not Canada are ^{93}Mo, ^{108m}Ag, ^{134}Cs, ^{166m}Ho, and ^{243}Am. This project will be specifically looking at these final five isotopes, which are a noted concern in the decommissioning of the FUGEN reactor, and attempting to determine the reason that they are a concern. Two of the isotopes which are of interest to Canada and not Japan listed above will also be examined, that of ^{121m}Sn and ^{41}Ca. Additional information on these isotopes and theories as to where they arise are discussed next. Theories are made with the help of my colleague Nicholas Somer (N. Somer, personal communication, February 26, 2020):

^{93}Mo

- Produced by neutron activation of ^{92}Mo. Likely from components that contain molybdenum alloys.
- Decays by electron capture which produces an X-ray with an average energy of 0.928 keV.
- A long half-life of 4000 years makes it a persistent source of x-rays.
- Each ^{93}Mo atom produces 11.5 X-ray photons on average per transformation with an average energy of 0.928 keV (Sowby, 1983).

^{108m}Ag

- A definitive source is hard to find, but is suspected to be neutron activation of ^{107}Ag.
- Pumps and other components in the heat transfer system have been found containing silver isotopes that have become activated, formed insoluble iodine salts, etc.
- A long half life of 418 years with a positron emission (91,3%) or gamma (8.96%) with 109 keV energy.
- Each ^{108m}Ag atom produces 2.78 gamma photons on average per transformation with an average energy of 578 keV (Sowby, 1983).

^{134}Cs

- The direct source of ^{134}Cs is as a fission product.
- Has a small Half-life of 2 years.

- Is also produced from neutron activation of stable ^{133}Cs, which is also a fission product.
- Each ^{134}Cs atom produces 2.23 gamma photons on average per transformation with an average energy of 698 keV (Sowby, 1983).

^{166m}Ho

- The source is likely as a product of neutron activation of ^{165}Ho, an observationally stable form of Ho.
- Beta decay into stable ^{166}Er. One metastable isotope of ^{166m}Ho has half-life of 185 μs, the other has a half-life of 1200 years.
- ^{165}Ho is a strong neutron poison, possibly used in safety system.
- Each ^{165}Ho atom produces 3.125 gamma photons on average per transformation with an average energy of 513 keV (Sowby, 1983).

^{243}Am

- Formed by neutron capture of ^{242}Pu.
- Increases exponentially over reactor lifetime from the successive neutron captures of ^{238}U.
- Has a 7370 year half-life with multiple decay chains.
- Undergoes a 5.27 MeV alpha decay to ^{239}Np, which beta decays to ^{239}Pu.
- Undergoes spontaneous fission.
- Each ^{243}Am atom produces 0.75 gamma photons on average per transformation with an average energy of 72.6 keV (Sowby, 1983).

^{121m}Sn

- Definitive Source is also difficult to ascertain, likely as an impurity in one of the core reactor materials.
- Likely a product of neutron absorption from ^{120}Sn.
- Each ^{121m}Sn atom produces 0.018 gamma photons on average per transformation with an average energy of 37.2 keV (Sowby, 1983).
- Unlike the other special isotopes, is found to be of interest to Canada and not Japan.

^{41}Ca

- Definitive Source is also difficult to ascertain, possibly arising from neutron activation of ^{40}Ca in concrete bioshield.
- Also has been shown to be of interest to Canada and not of interest to Japan
- Each ^{41}Ca atom produces 3.853 X-ray photons on average per transformation with an average energy of 0.13 keV (Sowby, 1983).

Chapter 3

Methodology

3.1 Use of Fuel Burnup to Gauge the amount of Isotopes Produced within the Fuel

Burnup is a way to measure how much uranium is burned in the reactor. It is the amount of energy produced by the fuel. Burnup is expressed in gigawatt-days per metric ton of uranium (GWd/MTU). Average burnup, around 35 GWd/MTU two decades ago, is over 45 GWd/MTU today. Utilities now are able to get more power out of their fuel before replacing it. This means they can operate longer between refuelling outages. It also means they use less fuel (United States Nuclear Regulatory Commission, 2018).

Fuel burnup increases the longer the fuel stays in a reactor, known as the fuel residency time. The longer fuel is burned, the more energy we get from the fuel in a bundle. However, the concentration of isotopes produced from the fuel also grows. When modelling a reactor, it is essential to try to match the refuelling period as much as

possible to real life in order for fuel to not burn either too much or too little and subsequently either produce too many or too few radioactive isotopes. Residency times for both the FUGEN and Pickering reactors can be seen in Table 3.1 (International Atomic Energy Agency, 1998, pg.8). From this, we can see that FUGEN has a fuel residency time of approximately three years, while Pickering, a CANDU reactor, should have a fuel residency of 320 d. Due to this, it is expected that FUGEN will have a higher burnup than Pickering.

Table 3.1:

Fuel Residence Times for Various Reactors

Reactor	Clad material	Clad operational mode	Max. LHGR, W/cm	Max. FGR, %	Fuel residence time
Atucha-1	Zry-4	free standing, pressurized, 1 7 MPa He	600 (design value for transients)	not applicable	195 EFPDs
BWR	Zry-2	free standing, pressurized with He	400-420	10-15	3-4 years
CANDU	Zry-4	collapsible, not pressurized	650 (design limit)	~10	average 320 EFPDs
FUGEN	Zry-2	free standing, pressurized, 0 1 MPa He	545	~10	app 3 years
RBMK	Zr-1%Nb	free standing, pressurized, 0 5 MPa He	485 (RBMK-1500)	~7	1100-1200 EFPDs

Note. The Table shows the properties of several nuclear reactors, including the CANDU and FUGEN reactors. From International Atomic Energy Agency (1998, pg.8). Copyright 1998 by International Atomic Energy Agency

There are several bundles within the FUGEN reactor with a varying number of fuel pencils (ranging from 28 to 37) and fuel enrichments of both MOX and regular UO_2. For the sake of this project, average values for both reactors will be taken from the literature. With regards to the burnup of the FUGEN reactor, an average reload burnup of 17 GWd/MTU will be used, which can be seen in Table 3.2. This is lower than the burnup values stated above; however, it is important to remember that FUGEN was a test reactor, with some fuel assemblies having much higher burnup than others and that, in general, burnup is affected by many factors, such as fuel residency time. The FUGEN burnup and other specifications can be seen in Table 3.2 (International Atomic Energy Agency, 1994, pg.51).

Table 3.2:

FUGEN and Other Advanced Test Reactor Specifications

Items	Unit	Fugen	D-ATR	C-ATR
Plant Output				
Thermal Power	MWt	557	1,930	3,125
Electric Power	MWt	165	606	1,000
Reactor Core				
Number of Pressure Tubes		224	616	648
Effective Core Height	m	3.7	3.7	4.5
Pressure Tube Inner Diameter	mm	117.8	117.8	117.8
Lattice Pitch	mm	240	240	240
Fuel				
Number of Fuel rods		28	36	48
Fissile material(reload)	wt%	2.0	3.3	4.0
Average Burn-up(reload)	GWd/t	17	31	48
Reactor Coolant System				
Number of Loops		2	2	2
Recirculation Flow	t/h	7,600	24,500	34,500
Steam Drum Pressure	bar	68	69	69

Note. The Table shows several properties of the FUGEN, D-ATR and C-ATR reactors. From International Atomic Energy Agency (1994, pg.51). Copyright 1994 by IAEA.

Burnup in the Pickering fuel is lower than in the FUGEN fuel as expected. About 1.25% of the uranium initially in the fuel bundle is converted to fission products and actinides while in the reactor (Wasywich, 1993). Burnup data can be seen in Table 3.3. Converting the fuel burnup of the Pickering bundle into the same units as FUGEN gives the Pickering fuel a burnup of 7.5 GWd/MTU. From this, we can see how much higher FUGEN burnup is compared to Pickering, and subsequently how much higher its fuel efficiency is, with the average burnup in the FUGEN reactor being double that of the Pickering reactor even in its lower burnup assemblies.

Table 3.3:

Composition of Irradiated Pickering Fuel

Fuel Burnup: 180 MW•h/kg U Cooling Time: 1 a	
Constituent	Percent of Original Total U
Unconverted ^{238}U	98.55
Unconverted ^{235}U	0.23
U converted to stable fission products	0.68
U converted to radioactive fission products	0.08
U converted to actinides (heavy nuclides)	0.46

Note. The Table shows the Burnup of fuel irradiated in the Pickering reactor after one year of cooling. From Mehta (1982, pg.11). Copyright 1982 by Atomic Energy of Canada Limited

3.2 Material Compositions Used in the Design of the MCNP Models

The radionuclides coming from neutron activation will originate in the materials used to construct the core. A thorough breakdown of the materials used in the reactor will therefore be necessary to produce an accurate simulation. If the data in Table 3.4 was originally given as a range of values, the average of that range is taken. The material compositions of the non-fuel materials used in the creation of the MCNP models can be found in Table 3.4 (Henderson, Anderson, Thomas, & Benton, 1997). The elements listed in the Table without specific isotopes selected are in their natural elemental form.

Table 3.4:

Composition (wt%) of non-fuel Reactor Materials Used in MCNP Models

Zircaloy-2	Cr-50 [0.004%]	Cr-52 [0.084%]	Cr-53 [0.01%]	Cr-54 [0.002%]
	Fe-54 [0.006%]	Fe-56 [0.092%]	Fe-57 [0.002%]	Fe-58 [0.0003%]
	Ni-58 [0.034%]	Ni-60 [0.013%]	Ni-61 [0.001%]	Ni-62 [0.002%]
	Ni-64 [0.0005%]	O-16 [0.12%]	Sn [1.4%]	Zr [98.23%]
Zircaloy-4	Cr-50 [0.004%]	Cr-52 [0.084%]	Cr-53 [0.01%]	Cr-54 [0.002%]
	Fe-54 [0.011%]	Fe-56 [0.184%]	Fe-57 [0.004%]	Fe-58 [0.001%]
	O-16 [0.12%]	Sn [1.4%]	Zr [98.18%]	
Zr-2.5	Nb-93 [2.5%]	Zr [97.5%]		
D_2O	H-1 [0.028%]	H-2 [19.95%]	O-16 [80.022%]	
Inconel-718	C [0.08%]	Si [0.35%]	P-31 [0.02%]	S [0.02%]
	Cr-50 [0.79%]	Cr-52 [15.90%]	Cr-53 [1.84%]	Cr-54 [0.47%]
	Mn-55 [0.35%]	Fe-54 [0.96%]	Fe-56 [15.44%]	Fe-57 [0.36%]
	Fe-58 [0.05%]	Ni-58 [35.38%]	Ni-60 [13.99%]	Ni-61 [0.62%]
	Ni-62 [1.99%]	Ni-64 [0.52%]	B-10 [0.001%]	B-11 [0.005%]
	Ti [0.90%]	Al-27 [0.50%]	Co-59 [1.00%]	Cu-63 [0.21%]
	Cu-65 [0.10%]	Nb-93 [2.56%]	Mo [3.05%]	Ta-181 [2.56%]
CANLUB	C [100%]			

Note. The material compositions of the non-fuel materials used in the creation of the MCNP models for FUGEN and Pickering are listed in the Table. Values for Zirc-2, Zirc-4, and Inconel-718 are adapted from Henderson et al. (1997, pg.9,153)

The composition of the D_2O in Table 3.4 is calculated knowing that the minimum required weight percentage of D_2O in reactor heavy-water is 99.75 wt% (Yan, Bromley, Dugal, & Colton, 2018) The weight concentrations are found using hand calculations and the assumption that the remaining 0.25% of the moderator is light-water. This is completed with the knowledge that the wt% of oxygen in heavy-water is 20% and in light-water is 88.8% (Williams, Gesh, & Pagh, 2006, pg.111).

Table 3.5:

Weight Percentages used in Modelling of Heavy-Water

Component	Allowable Percent (%)	Oxygen (wt%}	Hydrogen (wt%)	Deuterium (wt%)
Heavy-Water	99.75	79.8	0	19.95
Light-Water	0.25	0.222	0.028	0
Total	100	80.022	0.028	19.95

Note. The Table shows the isotopic breakdown of the heavy-water used in the modelling of the Pickering Reactor. Information on wt% in water from Williams et al. (2006, pg.111)

As part of the modelling of the Pickering and FUGEN reactors, the densities of each of the materials in Table 3.4 need to be specified. The material densities are listed in Table 3.6. Within the model the CANLUB is modelled as reactor-grade graphite.

Table 3.6:

Densities of Materials Used in MCNP models

Material	Density (g/cm^3)
Light-water	1
Heavy-water	1.11
Natural UO2	10.6
MOX Fuel	10.27
Zircaloy-2	6.56
Zircaloy-4	6.56
Zircaloy-2.5Nb	6.44
Inconel-718	8.19
CANLUB	1.7

Note. The Table shows the densities of the materials specified in the creation of the Pickering and FUGEN models. The density of Zirc-2.5Nb comes from MatWeb: Online Materials Information Resource (n.d.). The densities of Zircaloy-2, Zircaloy-4 and Inconel 718 come from Henderson et al. (1997, pg.9, 153). The density of the MOX fuel comes from Kato and Miyawaki (1976, pg.28). The density of the natural uranium fuel comes from Hastings (1982), as cited in Wasywich (1993, pg.68). The density of heavy-water comes from The Engineering ToolBox (2017)

3.3 Fuel Parameters Used in the Design of the MCNP Models

The Pickering and FUGEN reactors use different fuels, which will be the most significant contributor to the differences found between their isotopic inventories.

Pickering (Natural UO_2)

The Pickering fuel pellets are sintered pellets of UO_2, placed in a Zircaloy-4 sheath. A thin coating of a graphite-based compound (called CANLUB) is applied to the inside surface of the sheath to mitigate the harmful effects of power ramps (Popov, 2014). The Pickering reactor uses natural uranium in the production of its UO_2 fuel. The fuel used in the Pickering reactor is natural UO_2 which has not undergone any form of enrichment. The common isotopic breakdown of natural UO_2 can be seen in Table 3.7 (Yan et al., 2018, pg.182). From this we can see that the fissionable content of the natural uranium dioxide, the ^{235}U, only makes up 0.627% of the total weight.

Table 3.7:

Standard Isotopic Breakdown of Natural Uranium Dioxide

Fuel type	Nuclide	Nuclide amounts (wt%)	Nominal density (g/cm^3)
NUO_2	U234	4.68E−03	10.0
	U235	6.27E−01	
	U238	8.75E+01	
	O16	1.18E+01	
	O17	4.79E−03	

Note. The Table shows the isotopic breakdown of natural uranium dioxide as well as its density. Adapted from (Yan et al., 2018, pg.182). Copyright 2018 by Canadian Nuclear Laboratories

FUGEN (MOX)

The calandria tube in FUGEN is made of Zircaloy-2, while the pressure tube is made of Zircaloy 2.5% niobium alloy (Zr-2.5Nb). In the inner rings of the reactor are gadolinia-bearing fuel elements where MOX surrounds Gd_2O_3 to reduce power mismatch between the fresh and irradiated fuels as gadolinium is now the most commonly used burnable poison in commercial reactors (International Atomic Energy Agency, 1994). According to the supply and demand of plutonium, the MOX loading ratio has been flexibly changed from 34 to 72%.

The primary fuel used in the FUGEN reactor is a MOX fuel, which contains a combination of both UO_2 and PuO_2. Information on the fuel composition of the MOX fuel used in FUGEN can be seen below in Table 3.8 (Kato & Miyawaki, 1976). Some of the fuel assemblies in FUGEN used entirely enriched uranium fuel (E.U). However,

these assemblies and other assemblies used to test specific fuel combinations are not modelled in this project as the goal is to compare an average FUGEN fuel assembly to that of Pickering, not ones explicitly used for testing. As a result, the weight fractions for the MOX fuel shown in the left column of Table 3.8 are used in the production of the model.

Table 3.8:

Fuel Composition FUGEN

Isotope	Weight Fraction in Fuel	
	Pu	E.U
U-235	0.006221	0.013222
U-238	0.868695	0.868266
Oxygen	0.118467	0.118512
Pu-239	0.003838	---
Pu-240	0.001588	---
Pu-241	0.000926	---
Pu-242	0.000255	---

Note. The Table shows the isotopic composition of the average MOX fuel being used in the FUGEN reactor, with MOX fuel in the left column and enriched UO_2 in the right column. From Kato and Miyawaki (1976, pg.28). Copyright 1976 by Power Reactor and Nuclear Fuel Development Corporation, Tokyo Japan

To understand the fuel compositions given in Table 3.8 it is important to know the layout of the FUGEN fuel assembly in regards to its higher and lower enriched areas. In order to reduce the lower power peaking in the fuel assembly, the fissile plutonium content of the mixed oxide fuel is set to 0.55 wt% for the 16 rods in the outer ring and 0.8 wt% for the inner 12 rods. This can be seen in Figure 3.1 below (Kato & Miyawaki, 1976, pg.10). The combined average of these 28 rods gives an average plutonium enrichment of 0.66 wt%. Summing the weight fractions of the plutonium shown in Table 3.8 also gives this enrichment of 0.66 wt%, so that a single material composition can be used in all of the rods during the simulation.

Figure 3.1:

Mixed Oxide Fuel Assembly of FUGEN

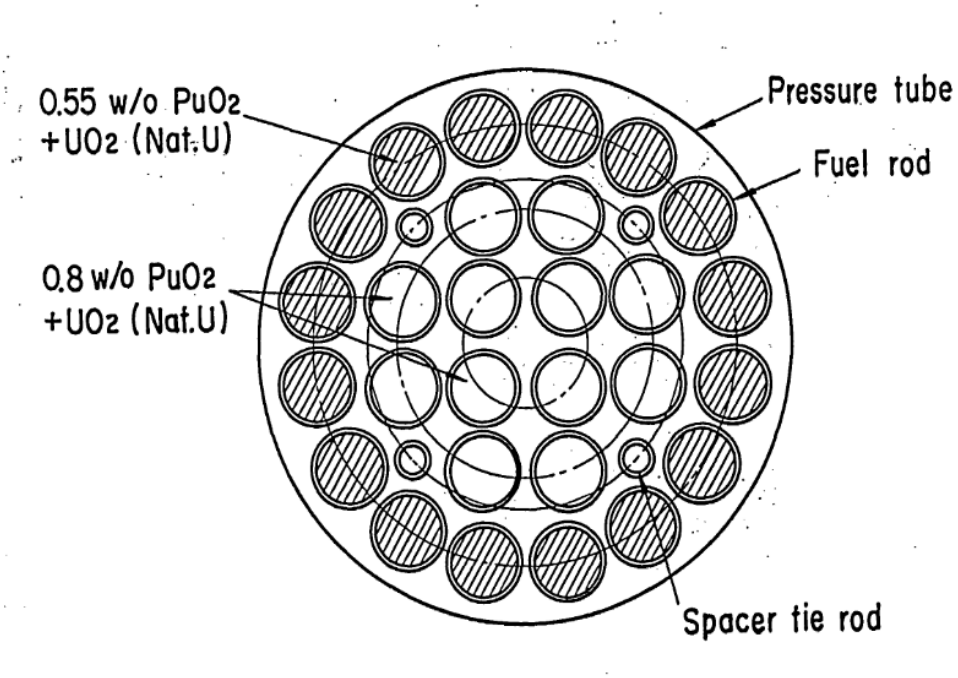

Note. The Figure shows the core layout of the average MOX fuel assembly of the FUGEN reactor. From Kato and Miyawaki (1976, pg.10). Copyright 1976 by Power Reactor and Nuclear Fuel Development Corporation, Tokyo Japan

3.4 Fuel and Other Dimensions Used in the Design of the MCNP Models

The models are incapable of accounting for leaks, so it is possible to model each reactor's bundles and from them gain an understanding of each reactor's isotopic inventory. This is because as no leaks are possible, any produced radioisotopes not be able to move from their original point of creation. A comparison of the fuels is accomplished by taking the number of fission products produced within the fuel and dividing it by the fuel volume to give an inventory per unit volume. For radioactive isotopes, this comparison will be made in Ci/cm^3, and when the nuclides of interest are nonradioactive, they will be displayed in g/cm^3. The model began with the modelling of a reactor bundle from Pickering. The dimensional data for both the Pickering bundle and FUGEN fuel assembly came from various sources, primarily from technical reports describing the characteristics and giving schematic drawings on the fuel bundles of the respective reactors (International Atomic Energy Agency, 1994; Ohtani et al., 2003; Wasywich, 1993) which will be discussed further in the subsequent sections.

3.4.1 Pickering

The dimensional data for the Pickering 28-element fuel bundle modelled in this project are from an Atomic Energy of Canada Limited (AECL) technical report on the characteristics of used CANDU fuel (Wasywich, 1993, pg.15, 68). The dimensional data for Pickering can be seen in Table 3.9 and Table 3.10. The difference between the data shown below and the model produced is that the UO_2 pellets in the model are connected into a singular, solid fuel rod with a length of 48 cm. While, in reality,

minor air gaps may exist between the pellets in a pencil, the results of this change in the final inventory should be negligible while reducing the amount of time spent programming the MCNP input file. In addition, a 0.01 mm thick coating of pure graphite to emulate CANLUB is also modelled on the interior of the pencils. 0.01 mm was chosen as no specific thickness of relevance could be found for CANLUB. For this research, the Pickering bundle was only modelled as a single bundle within a calandria tube filled with D_2O extending 10 cm past the bundle ends in either direction.

Table 3.9:

Dimensional Data for 28-element Pickering Fuel Bundle

Fissionable Material	Sintered pellets of natural UO_2
Structural Material	Zircaloy-4
UO_2 Pellet	
Outside diameter, mm	14
Length, mm (19)	23
(2)	22
Dish depth, mm	0.6
Land width, mm	0.3–0.5
Stack length, mm	480
Average density, Mg/m^3	10.6*
No. per element	21
End Plate	
Diameter, mm	88
Thickness, mm	1.6
Cladding	
Average inside diameter, mm	14
Average wall thickness, mm	0.4
Length, mm	486

Note. The Table contains unpublished data from J.L. Crosthwaite which is published by Wasywich. From Wasywich (1993, pg.15). Copyright 1993 by Atomic Energy of Canada Limited

Table 3.10:

Additional Dimensional Data for 28-element Pickering A Fuel

Fuel Design	-	Pickering A production
Fuel Identification	-	Bundle 10224C
Enrichment	-	Natural
Where Irradiated	-	Pickering A, Unit 1, L18W06
Fuel Density	-	10.6 Mg/m^3
Fuel Pellet Diameter	-	14.26 mm
Fuel Cladding	-	Zircaloy-4, 0.38 mm thick
Reported Linear Power	-	50 kW/m
Grain Growth, r/a	-	0.38 (grain radius/pellet radius)
Calculated Linear Power	-	51 kW/m
Burnup	-	223 MW•h/kg U
Comments	-	Constant heat rating throughout the duration of the irradiation
	-	Circumferential and radial cracking

Note. This table shows additional data which is specific to the Pickering A reactor being modelled. The Table contains data from Hastings (1982), as cited in Wasywich (1993, pg.68). Copyright 1993 by Atomic Energy of Canada Limited

The fuel is represented as macrobodies surrounding each other in the model and is built from the base up as cylinders, with each new surface bounding the previous surface, providing a new material and volume. The fuel pencils are the smallest unit and are composed of the natural UO_2 fuel. Surrounding this fuel is a 0.01 mm thick coating of CANLUB, which is modelled as pure elemental carbon. The Zircaloy-4 sheath surrounds the CANLUB with a thickness of 0.39 mm. In Table 3.9 an average wall thickness of 0.4 mm is shown for the cladding, but this is reduced in the model to a thickness of 0.39 mm to account for the added layer of CANLUB, while giving the same outer dimensions of the fuel pencil. This reduction of 0.01 mm from the thickness of the Zicraloy-4 sheath makes the model match the in-between point between the thickness shown in Table 3.9 of 0.4 mm and in Table 3.10 that shows the fuel cladding to have a thickness of 0.38 mm. The pellet diameter used in the model is 14.26 mm

from Table 3.10, as the value of 14 mm specified in Table 3.9 comes from unpublished data. Further information necessary for the production of the model is the dimensions of the pressure tube. The pressure tube within a CANDU reactor has an inner diameter of 103.4 mm and a thickness of 4.2 mm (Canadian Nuclear Safety Commission, 2018, slide.7)

The 28-elements within the bundle are modelled partially using a lattice and partially by hand when the lattice causes the outer fuel pins to overlap with the calandria tube and cause boolean errors. A cross-section of the bundle is shown in Figure 3.2. The use of the lattice function (LAT) as well as the FILL command is shown as the square grid at the centre of the Figure. This lattice allows for the replication of already made surfaces and shortens programming times.

This lattice structure is created by designating a large rectangular prism to contain the lattice. This region is then split into a grid based on the requirements and orientations of the model. This grid can be hexahedral (six faces) or hexagonal (eight faces). After designing the lattice, the element is chosen, which will be the (0,0,0) location in the lattice which will determine in which direction the lattice will be replicated. In the cell card, individual cells can be grouped into universes in order to group cells together for the purpose of replication. The FILL card in MCNP will then allow for the designated lattices to be filled with a desired cell or collection of cells. Figure 3.2 shows the hexahedral, or square, lattice used in the production of the model.

Figure 3.2:

Vertical Cross-Section of 28-element Pickering Fuel Bundle Showing Lattice

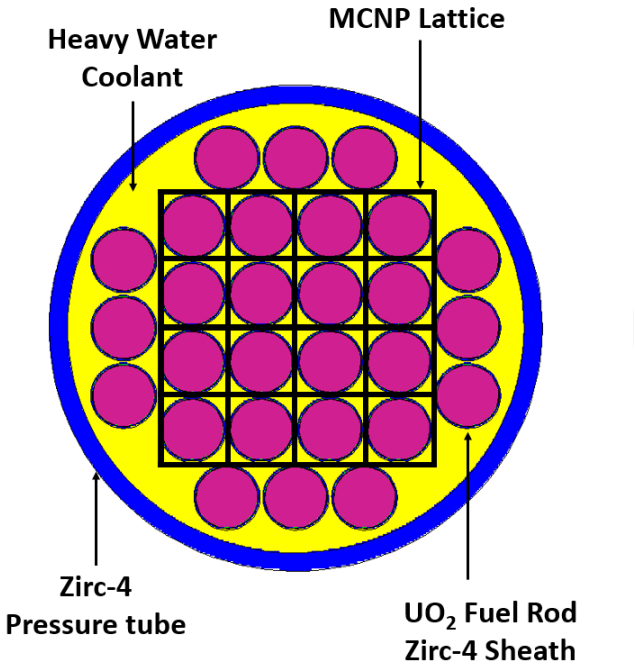

Note. The cross-section of the 28-element Pickering fuel bundle is generated from the MCNP input using the MCNP6 plotter with the lattice structure edited further in Microsoft PowerPoint

The outer 12 pencils in Figure 3.2 are modelled by hand as the use of the lattice function with a grid large enough to model all 28 pencils causes overlap with the calandria tube, causing boolean issues in the model. A vertical cross-section of the Pickering fuel bundle showing the length of the bundle and indicating the materials used is shown in Figure 3.3.

Figure 3.3:

Vertical Cross-Section showing side view of 28-element Pickering Fuel Bundle

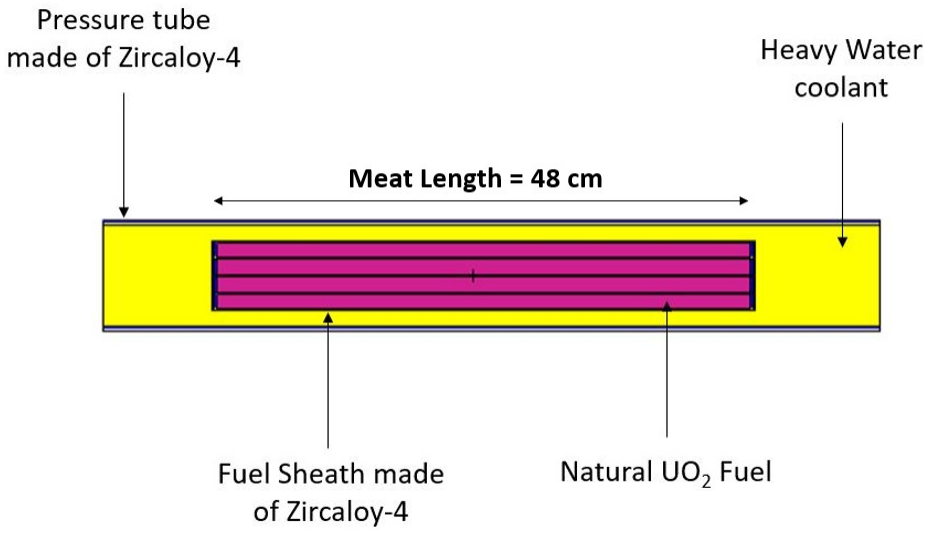

Note. The cross-section of the 28-element Pickering fuel bundle is generated from the MCNP input using the MCNP6 plotter and shows the material specifications of the model

Several model parameters were specified in section 3.4.1. The dimensions of the fuel assembly of the Pickering A reactor were taken from Table 3.9. The weight fractions of the natural UO_2 fuel were taken from Table 3.7. The fuel residency time was taken from Table 3.1 and the other material compositions were taken from Table 3.4. Given the net unit electrical output power of Pickering A of 515 MW(e) and a unit efficiency of 0.2579%, the thermal power of Pickering A is found to be 1996.8 MW(t) (Gilbert, 2016). Dividing this value by the 4680 bundles within Pickering A gives a bundle power of 426.6 kW. With this knowledge in addition to the fuel residency time of CANDU reactors from Table 3.1 of 320 d give the burnup parameters used in the Pickering model.

3.4.2 FUGEN

The dimensional data for the FUGEN reactor also comes mainly from technical documents (International Atomic Energy Agency, 1994; Ohtani et al., 2003). Unlike the Pickering reactor in which the fuel is divided into many bundles, the FUGEN reactor is modelled as an entire fuel assembly, with a total fuel length (Meat length) of 3.7 m compared to the relatively small size modelled in the Pickering reactor, which is only 0.48 m in length. Several differences other than the scale of the FUGEN model also exist that differentiate FUGEN from the Pickering model. There is no CANLUB graphite layer present in the FUGEN model, and as such, the dimensions of the model are exact to the specifications found in (International Atomic Energy Agency, 1994).

The FUGEN model contains a wider variety of materials and is physically larger than the Pickering model. FUGEN is light-water cooled rather than heavy-water cooled and uses both enriched uranium and plutonium, which create complex material and fuel specifications as discussed previously. Unlike in Pickering, the calandria tube and sheath materials are different. The sheath material within the FUGEN reactor is Zircaloy-2, while the calandria material is Zr-2.5Nb.

The FUGEN model also differs from the Pickering reactor in that it contains eight spacer tie rods, also made of Zircaloy-2. Also present within the FUGEN model are twelve spacers held together by these tie rods, which are made of Inconel-718 (Ikusawa, Kikuchi, & Ozawa, 2005). Positional data on the Inconel-718 spacers could not be found, so they were spread out evenly across the length of the fuel. Dimensional data for the spacers themselves could also not be found and were estimated from images of the spacers. The dimensions of these spacers would need to be more accurately specified to make the model as realistic as possible, but these estimates should be satisfactory for this project. Figure 3.4 shows a picture of the 37-Element EO9 Fuel

assembly which features much higher enrichment levels than is typical of the FUGEN reactor (Ikusawa et al., 2005). For this model, Figure 3.4 is only used to give a scale to the spacers with regard to the width of the pencils. The spacers appear to be wide enough to surround the elements and are estimated to be approximately 2 cm in thickness. This is how the Inconel-718 spacers are modelled in MCNP and can be seen in Figures 3.5 and 3.6. There are also four tie rods made of Zircaloy-2 with inner radii of 0.28 cm and outer radii of 0.35 cm (Kato & Miyawaki, 1976, pg.29).

Figure 3.4:

37-Element FUGEN EO9 Assembly Showing FUGEN Style Spacers

Note. The picture of the E09 Assembly shows the relative size of the Inconel-718 spacers relative to the fuel diameter and has been rotated to better fit in the page. From Ikusawa et al. (2005, pg.24). Copyright 2005 by Japan Nuclear Cycle Development Institute

The technical specifications for the generaly assembly of the FUGEN reactor can be seen in Table 3.11 (International Atomic Energy Agency, 1994, pg.96). Further specifications are found in Table 3.12 from the same paper (International Atomic Energy Agency, 1994, pg.98).

Figure 3.5:

Horizontal cross-section of FUGEN Assembly showing modelling of Inconel-718 spacers

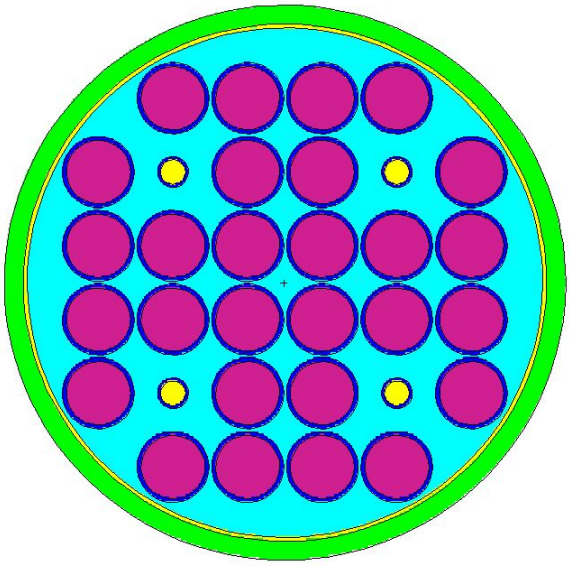

Note. The Figure shows the horizontal cross-section of the FUGEN fuel, showing the Inconel-718 spacers surrounding the fuel rods and spacer tie rods

Figure 3.6:

Vertical cross-section of FUGEN Assembly showing modelling of Inconel-718 spacers

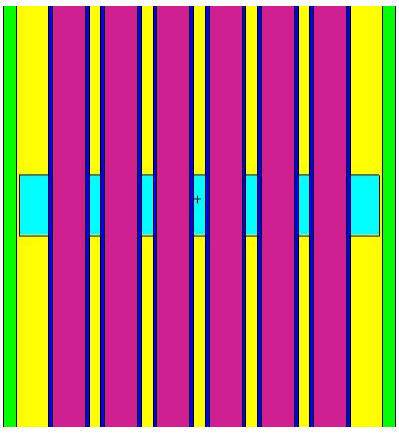

Note. The Figure shows the vertical cross-section of the FUGEN fuel, showing the Inconel-718 spacers height in comparison to the fuel rods

Table 3.11:

Dimensional Data for 28 Element FUGEN Fuel Assembly

Reactor type	Heavy-water-moderated,boiling-light-water-cooled, pressure-tube-type	
Output	Gross thermal output	557MWt
	Gross electrical output	165MWe
Core	Core height	3,700 mm
	Core diameter	4,050 mm
	Lattice	240 mm Square lattice
	Number of fuel channels	224
	Fuelinventory	34 t as metal
Fuel	Fuel material	MOX type A (%Pu fiss.) 0.8/0.8/0.6 MOX type B (%Pu fiss.) 1.6/1.6/1.1 UO2 type A (%235U) 1.5/1.5/1.5 UO2 type B (%235U) 1.9/1.9/1.9
	Pellet diameter	14.4 mm
	Fuel assembly	28 rods, 12 spacers
	Total length of fuel assembly	4,388 mm
	Cladding material	Zircaloy-2
	Cladding thickness (min.)	0.8 mm
Pressure tube	Material	Zr-2.5wt%Nb alloy
	Inner inside diameter	117.8 mm
	Thickness	4.3 mm
	Length	5 m
Steam drum	Diamete	2 m
	Length	16 m
	Material	Low carbon steel clad with stainless steel
Calandria tube	Material	Zircaloy-2
	Inner inside diameter	156.4 mm
	Thickness	1.9 mm

Note. The Table lists the dimensions of the fuel assembly of the FUGEN nuclear reactor used for the production of the FUGEN model and shows only part of the original Table. From International Atomic Energy Agency (1994, pg.96). Copyright 1993 by International Atomic Energy Agency

Table 3.12:

Additional Dimensional Data for 28-Element FUGEN Fuel Assembly

Item	Standard fuel ass.
Pellet	Type A B
Fissile content	MOX fuel w/o w/o
	Inner rod 1.5 2.3
$^{235}U+Pu$	Inter.rod 1.5 2.3
	Outer rod 1.3 1.8
	Average 1.4 2.0
	UO2 fuel
	All rods 1.5 1.9
Diameter (mm)	14.4
Clad	
Material	Zircaloy-2
Outer dia. (mm)	16.46
Spacer Material	Inconel
Number	12
Assembly	Inner rod 4
Number of fuel rods	Inter. rod 8
	Outer rod 16
	Total 28
Total length (mm)	4,388
	(Meat length 3,700)
Total weight (kg)	230

Note. The Table lists additional dimensions of the fuel assembly of the FUGEN nuclear reactor used for the production of the FUGEN model and shows only part of the original Table. From International Atomic Energy Agency (1994, pg.98).

Similar to how the model of the Pickering reactor was created, the dimensional data was modelled into MCNP using the lattice function described previously. It is important to remember that FUGEN is a vertically oriented reactor, so the images produced are now horizontal cross-sections rather than vertical like in the Pickering section. A horizontal cross-section of the FUGEN fuel assembly showing the lattice structure can be seen in Figure 3.7.

Figure 3.7:

Horizontal Cross Section of 28-element FUGEN Fuel Bundle Showing Lattice

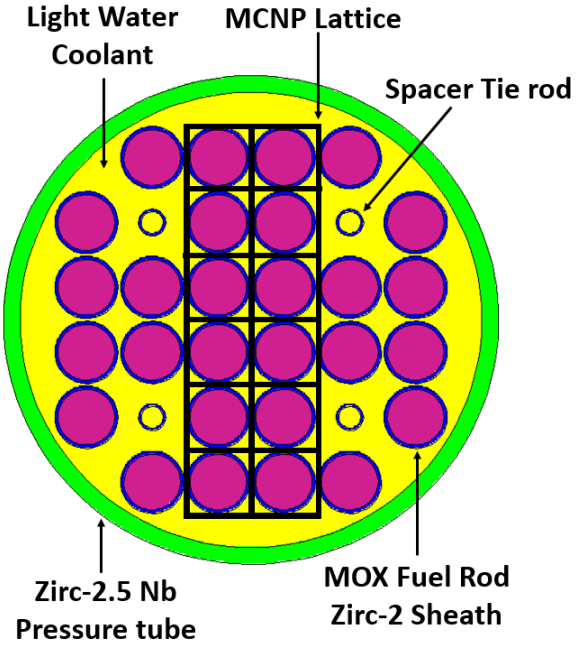

Note. The cross-section of the 28-element FUGEN fuel assembly is generated from the MCNP input using the MCNP6 plotter with the lattice structure edited further in Microsoft PowerPoint

Figure 3.7 resembles the model produced for the Pickering reactor seen in Figure 3.2. Within the FUGEN reactor, the presence of the spacer tie rods make the lattice function more difficult to implement, and more of the fuel pencils must be input into the model by hand. A side view of the model with indicated materials can be found in Figure 3.8.

Figure 3.8:

Vertical Cross-Section of 28-element FUGEN Assembly

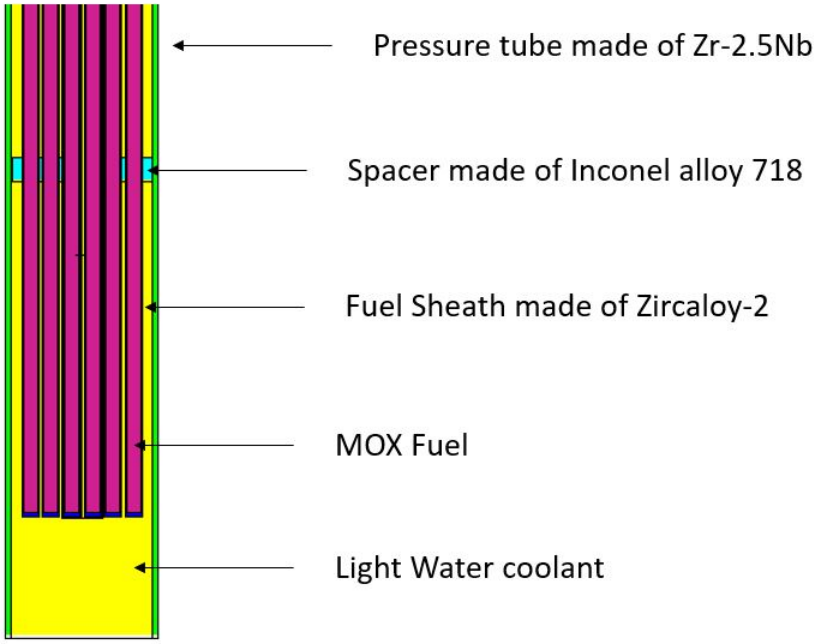

Note. The cross-section of the 28-element FUGEN fuel assembly is generated from the MCNP input using the MCNP6 plotter and shows the material specifications of the model

Several model parameters were specified in section 3.4.2. The dimensions of the fuel assembly of the FUGEN reactor were taken from Table 3.11. The weight fractions of the MOX fuel was taken from Table 3.8. The fuel residency time was taken from Table 3.1 and the other material compositions were taken from 3.4. The burn period set for the FUGEN model was three years from Table 3.1 with a total recoverable

fission power of 2.487 MW. The power under which the FUGEN model was run was found by dividing the gross thermal output of 557 MWt by the 224 fuel channels to get a "bundle power" of 2487 kW. The cladding thickness is taken from (Ohtani et al., 2003, pg.960) to be 0.9 mm.

While it is unnecessary to use as many KSRC locations as are described in the FUGEN model, see appendix B, the considerable length of the rods cause MCNP to spend several cycles increasing the size of the source distribution, and setting additional points along the length of the material can decrease these early wasted steps, increasing the speed of the program.

3.5 Geometric Verification of Models

Comparisons were made to published images and schematics of the fuel bundles being modelled for the purpose of verification. A side-by-side comparison of the Pickering 28-element fuel bundle and a reference model from (Wasywich, 1993, pg.4) can be seen in Figure 3.9.

Figure 3.9:

Comparison of Modelled Pickering Fuel Bundle to Schematic Drawing

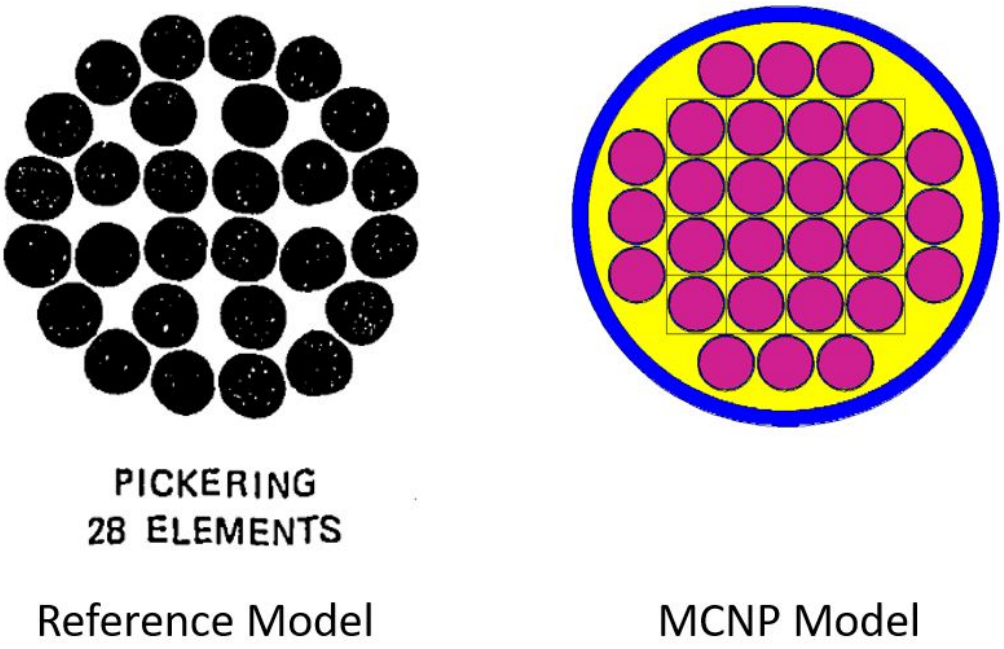

Note. The reference schematic shown on the left is compared to the vertical cross-section produced by the MCNP visual plotter using the Pickering model. Reference model from Wasywich (1993, pg.4). Copyright 1993 by Atomic Energy of Canada Limited

The comparison between the MCNP model and the reference model helps to confirm the fuel geometries used in the creation of the MCNP model. The MCNP model has a grid based rectangular orientation whereas the reference model is circular, this is due to the hexahedral lattice employed in the creation of the MCNP model. It is unlikely that this variation would cause considerable differences during when comparing the output of the burnup calculations as both models have this grid pattern, and will equally be affected by any variations caused by the rectangular orientation. As this work aims to compare the FUGEN and Pickering models, both models matching in this way should not affect the final comparison as the output of both models will be affected in the same way. A comparison of the FUGEN model to a schematic drawing, similar to the one made in Figure 3.9, can be seen in Figure 3.10 (Ohtani et al., 2003, pg.961).

Figure 3.10:

Comparison of Modelled FUGEN Fuel Bundle to Schematic Drawing

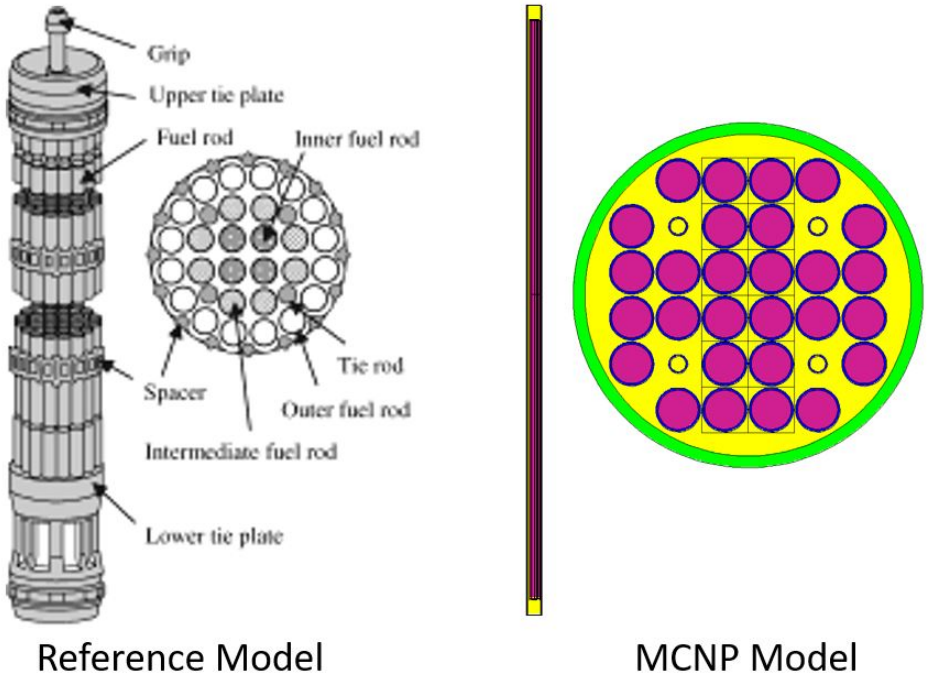

Note. The reference schematic shown on the left is compared to the horizontal cross-section produced by the MCNP visual plotter using the FUGEN model. Reference model from Ohtani et al. (2003, pg.961). Copyright 2003 by Taylor and Francis

The FUGEN model shows a similar parallel between the reference and the MCNP model, which helps confirm the model's geometries. The MCNP models for both reactors are simplified versions of the reference models. The MCNP models produced in this work do not contain several of the components shown in Figure 3.10 such as tie plates or shield plugs. These smaller components may need to be modelled if their material compositions are shown to have an active role in producing the isotopes of interest.

3.6 Input of Parameters into MCNP

The parameters of the MCNP models discussed in the previous sections need to be programmed into the MCNP input file in order for the depletion calculations to be performed. This will involved inputting the previously discussed fuel parameters into the three types of MCNP cards discussed in sections 1.7 and 1.8. The MCNP input files can be found in Appendix A and B.

3.6.1 Pickering

The Pickering fuel bundle is modelled as 28 fuel pencils, oriented in a grid pattern as shown in Figure 3.9 to resemble the reference schematics of the Pickering fuel bundles. While the FILL card in MCNP can be used to automatically copy several of the fuel pencils, the outer pencils are modelled by hand as to not cause boolean errors with the inner wall of the pressure tube, as the grid pattern would overlap the boundary of the pressure tube. As a result, it is required that 12 of the pencils are modelled separately from the FILL command. In addition to this, the separate fuel pellets are modelled as a solid fuel cylinder rather than individual pellets and have a meat length of 48 cm, coming from the pellet stack length in Table 3.9 of 480 mm.

Cell Card

In the cell card, the orientation of the regions and the material specifications of those regions is designated. There are six major cells being modelled in the Pickering fuel bundle. These are the fuel, the CANLUB layer, the Zirc-4 sheath, the pressure tube water, the Zirc-4 pressure tube, and then the universe outside of the pressure tube. As discussed earlier, the three cells of the fuel, CANLUB, and fuel sheath are modelled 28 times within the code but are programmed identically into MCNP, with the only difference being their location.

The basic structure of the cell card uses the fuel as the smallest cell from which the model grows outward. As macrobodies are implemented in the surface card. It is possible to define the regions in the cell card as either inside or outside of the 3D-shapes described by the macrobody. The fuel is defined as everything within the first cylinder described in the surface card. Everything between the fuel cylinder and the cylinder describing the inner edge of the sheath is CANLUB. The sheath is then defined as the region between the cylinders describing the inner and outer edges of the sheath and is made of Zircaloy-4. This Zircaloy-4 cylinder which contains the fuel and CANLUB is defined as a fuel pencil and is copied 28 times within the Pickering model. The region outside of the fuel pencils and inside the inner wall of the pressure tube is defined as heavy water. The region between the cylinders that define the inner and outer walls of the pressure tube is the pressure tube. The final region defined in the cell card is the region outside of the outer wall of the pressure tube and is defined as a void through which particle transport is not performed. The densities of each of the cells are also specified in this card, and are retrieved from Table 3.6. The volumes of these cells are also defined in the cell card and are derived from the surfaces described in the surface card. The calculation of these volumes is described in the next section.

Surface Card

In the surface card, the shape and dimensions of the model are defined. In the modelling of the Pickering reactor, the only macrobodies used are the right circular cylinder (RCC), and the arbitrarily oriented orthogonal box (BOX). The dimensions used in the production of the Pickering model come from Table 3.9 and Table 3.10.

As stated previously, the fuel is modelled as an RCC. From Table 3.9 the fuel diameter is taken as 14.26 mm, however as the RCC in MCNP deals with radii, not diameters, and use cm, not mm, this is modelled as an RCC centred on the Y/Z axis, extending 48 cm in the X-direction with a radius of 0.713 cm. The CANLUB is modelled as an RCC centred on the Y/Z axis, starting 0.001 cm to the left of the fuel, and extending 48.002 cm in the X-direction with a radius of 0.714 cm. This gives the CANLUB a thickness of 0.001 cm in all directions surrounding the fuel. The fuel sheath is centred on the Y/Z axis and is situated 0.039 cm to the left of the CANLUB cylinder, and extends 48.08 cm in the X-direction with a radius of 0.753 cm. This gives the sheath a thickness of 0.039 cm in all directions surrounding the CANLUB, as described in section 3.4.1. These three surfaces together are a fuel pencil and are then grouped together as universe 1 in order to be copied in the FILL card.

In order to copy the fuel pencils, it is necessary to define a square grid pattern into which the pencils are copied. Using the pencil diameter of 1.506 cm, it was decided that the grid would be made of squares with a side length of 1.56 cm. This was created in MCNP using the BOX macrobody, with side lengths of 6.24 cm in the Y/Z direction, and a length in the X-direction just large enough to encompass the fuel pencil. The length was chosen to be 0.1 cm larger than the fuel sheath on either side of the X-direction. This large BOX was then split into a grid of 16 smaller boxes with side length of 1.56 cm within the centre of the pressure tube, with no overlapping

boundaries. The side length was chosen using the MCNP visual editor as to best resemble the reference schematics while not causing boolean issues with the inner wall of the pressure tube. The remaining 12 rods were modelled individually within MCNP, but still follow the grid pattern, with the distance between the centre of adjacent fuel pencils remaining at 1.56 cm.

The next surfaces described are the inner and outer walls of the pressure tube. The inner wall of the pressure tube is modelled as an RCC centred at the middle of the grid pattern, which based on the geometries described is located at (2.34, 2.34) on the Y/Z axis. From this centre point on the Y/Z axis, the inner wall of the pressure tube is defined as an RCC with a radius of 5.17 cm, starting 10 cm past one side of the bundle and extending along the X-axis for 68 cm, as to extend 10 cm past the fuel bundle on both sides. The outer wall of the pressure tube is modelled similarly to the inner wall, but with a radius of 5.59 cm due to its stated thickness of 0.42 cm in section 3.4.1. Now with all the surfaces input into MCNP, the respective volumes for the cells are calculated. This is accomplished by using equation 3.1, the volume of a cylinder given by:

$$V = \pi r^2 h \tag{3.1}$$

where r is the radius of the cylinder, and h is the height of the cylinder. The volume of a cell is found by applying equation 3.1 to any of the RCC surfaces, and subtracting any inner volumes from the calculated volume. An example of the calculation of the CANLUB volume is shown by:

$$V_{CANLUB} = V_{CANLUBSurface} - V_{FuelSurface}$$
$$V_{CANLUB} = \pi r^2_{CANLUB} h - \pi r^2_{Fuel} h$$
$$V_{CANLUB} = \pi(0.714cm)^2(48.002cm) - \pi(0.713)^2(48.0cm)$$
$$V_{CANLUB} = 0.2184cm^2$$

The volumes important to the model are calculated in excel using equation 3.1 and are listed in Table 3.13.

Table 3.13:

Densities Calculated for the Pickering MCNP Input File

Cell	Fuel Volume (cm^2)
UO_2 Fuel	76.6602
CANLUB	0.2184
Zirc-4 Sheath	8.7668
Fuel Pencil	85.6454
Heavy Water	3311.9769
Pressure Tube	3363.5016

Note. The Table lists the volumes of the cells calculated for the Pickering fuel bundle

Being able to insert the cell volumes into the cell card is useful when you want the cell volume to be a specific value, however MCNP will automatically calculate cell volumes based on the input file, so assuming there are no boundary issues in the MCNP input file, it is not necessary to input the volumes manually. With the cells and surfaces defined, it is possible to order MCNP to perform the desired calculations.

Data Card

The data card is where the specific commands for the MCNP file are input. The first command given in the data card is to turn physics models on and to set the neutron activation to always use models. This tells MCNP to use models when delayed neutrons are produced, rather than looking up values in the library. This is useful when looking at a wide variety of isotopes, some of which may not have reference values listed in the library.

In the research the default values for the KCODE card are used. The recommended value of 10000 neutrons per history, running 150 histories and discarding the first 50 is used. The default is to discard the first 30 but early tests of the models showed it often took past the original 30 for the values to stabilize, so it was decided that the first fifty runs of the model would be discarded. In the KSCR card the triple locations of fission points used to start the chain reaction are defined. All that is required for the KCODE is a minimum of one source point within each fuel region, but adding more points can cause less of the original runs to be discarded, as the model will spend less time growing the burn region to fit the entirety of the fuel.

Within the BURN card the values specific to the Pickering model are input. Based on Table 3.1, a burn time of 320 d is retrieved from the listed fuel residence times. A total recoverable fission power of 0.426 MW is defined, which is derived from the discussion in section 3.4.1. In the BURN card, the materials you wish to perform burnup calculations and neutron activation on are chosen. In the Pickering model, the fuel and the Zirc-4 sheath are chosen. Their respective total volumes need to be input for the calculations to be completed. For the decided materials all that is required it to multiply the values in Table 3.1 by 28 to represent the number of individual rods. The calculated total material volumes are 2146.49 cm^3 and 245.47 cm^3 respectively

for the fuel and sheath volumes. In the BOPT card the specifics of isotope selection for the burnup calculations are performed. The first variable in the BOPT card is the Q value multiplier and is left as its default value. The second variable within the BOPT card specifies the tier of the burnup as well as the order which the results are specified. In MCNP, the tier chosen will determine how many isotopes you want to be considered within the caolculations. Tier 1 only includes a very limited number of nuclides whereas tier 3 contains the entirety of the list of nuclides in MCNP. Within the Pickering model, tier 3 which contains the most fission products is chosen as many of the desired isotopes are uncommon and not included in the more limited tier. The third variable in the BOPT card specifies that CINDER90 will be allowed to calculate 1-group cross-sections for any nuclides encountered by the program that do not contain tabular data.

The final specifications made in the data card and the input file at large is defining the material compositions in wt% of the materials used within the model. The values used in this section of the data card are taken directly from Table 3.4 and Table 3.7.

3.6.2 FUGEN

The FUGEN model is generated similarly to the Pickering Model. The FUGEN model is physically larger than the Pickering model, and while it doesn't contain a layer of CANLUB, it does contain both Inconel-718 spacers as well as 4 tie rods that run the length of the fuel assembly. In the FUGEN model, the FILL card is used to automatically copy 12 of the fuel pencils into a pre-determined grid. As a result, the remaining 16 pencils are modelled manually outside of the FILL card. The fuel in the FUGEN model is also modelled as a solid cylinder of fuel with a total meat length of 370 cm.

Cell Card

The orientations of the cells are similar to that of the Pickering model described previously. In the FUGEN model there are seven major cells being modelled, these being the fuel, sheath, tie rods, pressure tube water, Inconel spacers, Zirc-2.5Nb pressure tube, and the void outside of the model. The basic structure of the FUGEN cell card also follows the Pickering model in that it is a series of cylinders, with the fuel as the basis of the model. Everything in the cylinder describing the fuel is made of MOX fuel. The region described as being between the outer edge of the fuel and the outer edge of the sheath is the Zircaloy-2 sheath. This Zircaloy-2 sheath which contains the fuel is then defined as a fuel pencil and is copied 28 times throughout the model. Four hollow tie rods are also included in the FUGEN model. As they are hollow, the region inside of the inner wall of the tie rod is defined as light water. The region between the inner and outer walls of the tie rod is the Zircaloy-2 tie rod. Twelve Inconel-718 spacers are further included in the model. The region within the Inconel spacers is defined as being within a solid cylinder describing the outer surface of the spacer, excluding the regions comprised of the 28 fuel pencils which pass through the spacer. The region outside of the fuel pencils, tie rods and Inconel spacers, but within the inner wall of the pressure tube is defined as the light-water coolant. The region between the surfaces describing the inner and outer wall of the pressure tube is defined as the Zr-2.5Nb pressure tube. The region outside of the outer wall of the pressure tube is defined as a void through which particles are not transported. With all of the cells defined, the surface card is programmed next.

Surface Card

In the surface card, the shape and dimensions of the regions of the model are defined. As was done in the Pickering model, the FUGEN model is made primarily of RCCs with a BOX used to copy 12 of the fuel pencils into a rectangular grid. The dimensins used in the modelling of the FUGEN reactor come from Table 3.11 and Table 3.12 with other parameters defined in section 3.4.2.

The fuel is once again modelled as an RCC. As the FUGEN reactor is a vertically oriented reactor, the RCCs are now oriented along the X/Y axis. The fuel within the FUGEN model is modelled as an RCC centred on the Z-axis with a radius of 0.72 cm, extending 370 cm in the Z-direction. The fuel sheath is then modelled as having a thickness of 0.09 cm in all directions surrounding the fuel. This is accomplished by placing the starting point of the sheath's RCC 0.09 cm below the fuel on the Z-axis, and extending along the Z-axis with a length of 370.18 cm and a radius of 0.81 cm. These two surfaces are grouped together as universe 1 in the cell card in order to be copied using the FILL card.

In order to use the FILL command, it is once again necessary to designate a BOX within the model which can be divided into a rectangular grid into which the pencils will be copied. Using a similar method as is described for the Pickering model, a BOX with side lengths of 3.38 cm and 10.08 cm in the Y/Z direction, with a length just large enough to fit the pencils within is generated. This Box is then divided into a 2X6 grid of 12 boxes with side lengths of 1.68 cm. This side length was chosen as to best resemble the reference schematic using the MCNP visual plotter while not causing boolean issues via boundary overlaps. The remaining 16 rods were modelled individually within MCNP, but still follow the grid pattern with the distance between the centre of the fuel bundles remaining 1.68 cm.

The next surfaces modelled in the surface card are the outer and inner walls of the tie rods. As described in section 3.4.2, the inner wall of the tie rods are defined as RCCs with lengths of 370.18 cm and radius of 0.28 cm. The outer wall of the tie rods are then defined as RCCs with lengths of 370.18 cm and a radius of 0.35 cm. The Inconel spacers are modelled as RCCs and are defined as having a radius of 5.8 cm and a length of 2 cm. The 12 spacers are evenly divided along the length of the fuel, with a distance of 27.5 cm between them.

The final surfaces defined are the inner and outer walls of the pressure tube. The inner wall is defined as an RCC centred on the middle of the grid, at (0.84, 4.2) in the Y/Z direction. The cylinder describing the inner wall of the pressure tube is set as being 10 cm below the fuel in the Z-direction with a length of 390 cm, giving a length of 10 cm past both sides of the fuel and a radius of 5.89 cm. The outer wall of the pressure tubes is similarly modelled as an RCC but with a radius of 6.32 cm. Using equation 3.1, the respective volumes of the cells are once again calculated. The cell volumes are listed in Table 3.14.

Table 3.14:

Densities Calculated for the FUGEN MCNP Input File

Cell	Fuel Volume (cm^2)
MOX Fuel	602.5826
Zirc-2 Sheath	160.4320
Fuel Pencil	763.0146
Tie Rod	51.2863
Light Water	21141.0847
Spacer	95.9392
Pressure Tube	6432.7785

Note. The Table lists the volumes of the cells calculated for the FUGEN fuel assembly

Data Card

The data card of the FUGEN reactor largely matches the Pickering data card. The KCODE card is identical, though more KSCR triplets are used in order to account for the FUGEN model which is much larger physically than the Pickering model. In the BURN card, the burn time, and recoverable power of the FUGEN fuel assembly being modelled are designated. From Table 3.1, the fuel residence time is taken to be 3 years, or 1095 d. A recoverable fission power of 2.487 MW is used as was defined in section 3.4.2.

The materials in the FUGEN model which are having burnup and neutron activation calculations applied to are the MOX fuel, the Zirc-2 sheath/tie rods, the Zr-2.5Nb pressure tube and the Inconel-718 spacers. The calulated total volumes for these materials are 16872, 4492, 6432, and 1151 cm^3 respectively. The final specifications made in the data card are the definitions of the material compositions used in the model in wt%. The values used in thhis section are taken directly from Table 3.4 and Table 3.8.

Chapter 4

Results/Discussion

This research aimed to model the Pickering and FUGEN reactors' fuel assemblies and compare their respective isotopic inventories before and after being fissioned. The produced MCNP models underwent depletion calculations, and their new isotopic inventories were calculated. MCNP created an extensive list of isotopes produced during the simulation using the inputs described in the methodology section. Based on the actinide and nonactinide inventories created by MCNP at the end of the depletion calculations, comparisons were made on the isotopes of interest whose activities have been calculated. In this section, these calculated isotopic inventories are examined and discussed.

4.1 Uncertainty

When analysing experimental data it is important to discuss the uncertainty in the results. This is equally true for the results of an MCNP analysis. Normally MCNP will provide a standard deviation with any printed results. "All MCNP calculations, normalized to per starting particle history (except for some criticality calculations), are printed together with the fractional standard deviation (fsd)" (Hussein, 2016, slide.78). This research however deals with the aforementioned criticality questions through which MCNP will not provide an fsd.

In order to include error in the results of the MCNP models, the output of the MCNP burnup calculations were treated as data points and further analysis was completed on them. The MCNP code was run five separate times each for Pickering and FUGEN models. The inventory values in curies and grams produced were recorded in each run and the averages and standard deviations of these runs were taken. All of the separate runs however produced identical results and the calculated standard deviation was zero.

While MCNP did calculate the final estimated k_{eff} to be 0.11791 with a standard deviation of 0.00028 for the FUGEN model and a value of 0.06435 with a standard deviation of 0.00009 for the Pickering model, these uncertainties cannot be applied to the final inventory values calculated using the MCNP libraries. As such the values listed in this section will not appear with uncertainty values.

4.2 Isotopic Inventory

When discussing the inventories calculated using the depletion codes with respect to decommissioning, it is crucial first to discuss the half-lives of the isotopes of interest. Even though MCNP may show an isotope as having a significant activity present in the calculated isotopic inventory, if that isotope has a short half-life, it may not be of substantial concern in decommissioning due to the techniques of delayed decommissioning discussed earlier. A condensed list of the half-lives of the isotopes of interest can be seen in Table 4.1.

Table 4.1:

Half-Lives of the Isotopes of Interest

Isotope	Half-Life (yrs)
Mo-93	4000
Ag-108m	418
Cs-134	2.06
Ho-166m	1200
Am-243	7370
Ca-41	130000
Sn-121m	50

Note. The half-lives of the isotopes chosen to be of interest to the decommissioning of nuclear reactors/facilities are listed in years.

The only isotope that has a half-life short enough to be of note to decommissioning is ^{134}Cs with its short two year half-life. Due to this short half-life, it is anticipated that it would decay away given a 20 or 30 year-long safe storage and surveillance period, largely reducing its possible danger. The output of the fuel inventories calculated by MCNP can be seen in Tables 4.2 and 4.3. Table 4.2 shows that the FUGEN reactor

does create more of the isotopes of interest; however, without normalization, the reactors cannot be directly compared to each other. It is important to remember that except for calcium and tin, most of these isotopes are of interest to Japan and not Canada, as can be seen in Table 2.2.

Table 4.2:

Calculated Radioactive Isotopic inventory

Isotope	Pickering 320-days (Ci)	FUGEN 3-Years (Ci)
Mo-93	0	6.46E-08
Ag-108m	0	0
Cs-134	2.25E+01	7.61E+03
Ho-166m	0	0
Am-243	0	3.32E+00
Ca-41	0	0
Sn-121m	0	0

Note. The values in the Table are calculated by performing burnup calculations on the previously described MCNP models and represent the radioactive isotopes chosen to be of interest. These values are the direct output of MCNP, averaged over 5 separate runs of the code, ± the standard deviation of those runs

Table 4.3:

Calculated Non-radioactive isotopic Inventory

Isotope	Pickering 320-days (g)	FUGEN 3-Years (g)
Ag-107	4.40E-08	3.04E-06
Ho-165	7.36E-05	1.70E-03
Sn-120	2.73E-02	3.32E-01

Note. The values in the Table are calculated by performing burnup calculations on the previously described MCNP models and represent the nonradioactive isotopes that when activated could become the isotopes of interest. These values are the direct output of MCNP, averaged over 5 separate runs of the code ± the standard deviation of those runs

Table 4.2 shows that many of the isotopes of interest do not appear in the MCNP models. However, the data shown in Table 4.3 may indicate why the metastable isotopes not found in the model may be of more interest to one regulator than the other. The isotopes seen in Table 4.3 are not listed isotopes of interest and are nonradioactive, which is why they are displayed in grams rather than in curies. While the models do not show these metastable isotopes, they show the creation of these nonradioactive isotopes that can then be activated to become them. These precursor isotopes can help make a similar comparison to the one done with the other isotopes found in the model directly. The other outlier in the model is ^{41}Ca, which is not found anywhere in either of the models. The reason for this is likely that the model does not extend to the concrete biological shield, which is where ^{41}Ca contamination is commonly expected due to neutron activation of ^{40}Ca (Hou, 2005).

There are many reasons why calcium and other isotopes are not produced within the model. While the fissioning of the fuels in MCNP can draw from the entire list of fission products to determine fission product yields, neutron activation in MCNP can only occur when the precursor isotopes that will be activated are modelled into the input file. For example, rare isotopes such as metastable silver in reactors can be produced through the neutron activation of trace silver impurities within metal alloys. However, without a thorough isotopic breakdown of the materials within the reactors, trace impurities are challenging to model and cannot be placed into the model without a definitive source and reason.

The locations where they arise in the model can be examined to differentiate whether these isotopes are produced via neutron activation or fission. Tables 4.4 and 4.5 show the isotopic inventories of the reactors split into the materials in which they are found.

Table 4.4:

sotopic Inventory of Pickering Model by Material

Isotope	Material 1 (NUO2) (Ci)	Material 2 (Zirc-4)(Ci)
Cs-134	2.25E+01	0
Ag-107	4.40E-08	0
Ho-165	7.36E-05	0
Sn-120	2.73E-02	0

Note. The Table shows the isotopic inventory of Pickering calculated using the MCNP models and specifies where these isotopes are located. Only the non-zero isotopes from Tables 4.2 and 4.3 are included.

Table 4.5:

Isotopic Inventory of FUGEN Model by Material

Isotope	Material 1 (MOX) (Ci)	Material 2 (Zirc-2) (Ci)	Material 4 (Zr-2.5 Nb) (Ci)	Material 5 (Inconel-718)(Ci)
Mo-93	0	0	4.52E-08	1.94E-08
Cs-134	7.61E+03	0	0	0
Am-243	3.32E+00	0	0	0
Ag-107	3.04E-06	0	0	0
Ho-165	1.70E-03	0	0	0
Sn-120	3.32E-01	0	0	0

Note. The Table shows the isotopic inventory of FUGEN calculated using the MCNP models and specifies where these isotopes are located. Only the non-zero isotopes from Tables 4.2 and 4.3 are included.

The majority of the isotopes are created within the fuel and can thus be categorized as fission products. The only special isotope present in the model that can be entirely categorized as arising from neutron activation is ^{93}Mo. Within the FUGEN model, approximately two-thirds of the ^{93}Mo is created within the calandria tube, and one third is produced within the Inconel-718 spacers. This is likely due to neutron activation of ^{93}Nb present in these materials.

The values in Tables 4.2 and 4.3 cannot be directly compared to each other without first normalizing them, and this is due to the fact that the FUGEN model is much larger than the Pickering model. As the majority of the isotopes of interest all appear within the reactors' fuel, it is possible to divide by the fuel volume of each reactor to find isotope production per cubic centimetre of fuel. This is not possible for the ^{93}Mo, but as none appears in the Pickering model, it is unnecessary to make that comparison.

Table 4.6:

Radioactive Isotopic Inventory of Fuel per Unit Volume

Isotope	Pickering (Ci/cm^3)	FUGEN (Ci/cm^3)	Ratio of FUGEN over Pickering
Cs-134	1.05E-02	4.51E-01	43.1
Am-243	0	1.97E-04	Infinite
Mo-93	0	Not in Fuel	N/A

Note. The Table shows the radioactive concentrations of the Pickering and FUGEN reactors after being normalized to their respective fuel volumes. ^{243}Am does not appear in the Pickering reactor so it considered that there is infinity more of it in the FUGEN reactor.

Table 4.7:

Nonradioactive Isotopic Inventory of Fuel per Unit Volume

Isotope	Pickering (g/cm^3)	FUGEN (g/cm^3)	Ratio of FUGEN over Pickering
Ag-107	2.05E-11	1.80E-10	8.8
Ho-165	3.43E-08	1.01E-07	2.9
Sn-120	1.27E-05	1.97E-05	1.5

Note. The Table shows the nonradioactive concentrations of the Pickering and FUGEN reactors after being normalized to their respective fuel volumes. As these are nonradioactive isotopes, they are in units of g/cm^3, rather than Ci/cm^3 like they are in Table 4.6.

The comparisons made in Tables 4.6 and 4.7 show that on a per fuel volume basis, the FUGEN reactor produced over 40 times the ^{134}Cs that the Pickering reactor does, and also produces ^{243}Am and ^{93}Mo, which are not shown to arise in the Pickering model at all. The presence of ^{93}Mo is explained above, and the ^{243}Am comes from the neutron capture of ^{242}Pu. The Pickering reactor utilizes NUO_2 fuel, and as such ^{243}Am was not expected to be present in the model, to begin with.

Burnup values are determined from the MCNP output for both the FUGEN and Pickering reactors fuels. The burnup calculated in the MCNP model of Pickering is 6.8 GWd/MTU. This burnup can be compared to the Pickering burnup data discussed earlier coming from Table 3.3. The reference Pickering fuel underwent an average burnup of 7.5 GWd/MTU. Having the calculated fuel burnup of the Pickering fuel similar to that of reference data helps verify and add credibility to the model.

MCNP calculates the burnup value in the FUGEN model as 17.8 GWd/MTU. This burnup can be compared to the FUGEN burnup values discussed earlier coming from Table 3.2. The reference average FUGEN fuel burnup value is 17 GWd/MTU. Once again, having a calculated burnup value be similar to that of the reference values increases the credibility of the MCNP model.

4.3 Discussion

4.3.1 Verification of Model

It is necessary to compare these inventories produced by the MCNP models with reference inventory data to verify the model and give the comparison value. One of the primary goals for this research is to create a model to simulate the FUGEN model as inventory values for the FUGEN reactor are unknown to us. If the inventory numbers for FUGEN were known, this research would be unnecessary as a simple comparison could be made with the published CANDU inventories. However, this makes a comparison of the model difficult, as the FUGEN model cannot be benchmarked. However, it is constructed similarly to the Pickering model, which does have reference data to compare against. If the Pickering model can be verified to a real model, this will also add validity to the FUGEN model by extension. Table 4.8 shows a choice of isotopes from both the Pickering MCNP as well as the reference data provided (Barber, 2013, 2014). A simple percent difference comparison is made based on a per bundle inventory.

Table 4.8:

Percent Difference Between Pickering MCNP and Reference Fuel Inventories

Isotope	Half-Life	Reference Data (Ci)	MCNP Model (Ci)	Percent Difference
I-135	6.57 h	22154	24500	-11%
Ba-140	12.75 d	20854	20200	3.14%
Cs-134	2.06 a	75	22.46	70%
Cs-136	13.16 d	167	93.72	44%
Cs-137	30.17 a	215	430.1	-100%
Pm-147	2.62 a	632	1745	-176%
Xe-133	5.25 d	22503	24120	-7.19%
Xe-135	9.14 h	1706	24900	-1359.55%

Note. The Table shows the comparison of an assortment of isotopes calculated using the Pickering MCNP model compared to reference data for the inventory of a Pickering A reactor. Reference data from Barber (2013, 2014)

Table 4.8 shows some correlation between the inventories of the Pickering bundles, but it is not ideal. It does not appear to be a difference in burnup value, as some of the elements are higher and some are lower than the reference model. In addition, the burnup values calculated within MCNP are similar to those of the reference values discussed in previous sections. The isotopes that produce the bulk of the radiation within the bundles also show a more significant correlation than those that produce only small amounts.

A possible reason for this difference may be that the reference data comes from dividing the total inventory of the reactor by the number of bundles. This comes with the assumption that all of the radiation within the reactor can be found within the bundles themselves, with the rest of the reactor being clear of radioactive sources. The MCNP model also assumes no leakage or discharge of the isotopes created within.

It is unknown if the reference reactor inventory comes from real-world data or models as well, and it is also unknown how long after shut-down, these values may be from. This will have a significant effect on those isotopes with a short half-life. For example, the ^{135}Xe has a very short half-life of only 9.2 hours, so despite how large the percent difference shown in Table 4.8 depicts, a difference of a day or two between measurements could lead to a similar percent difference. ^{147}Pm also had a relatively short half-life of 2.6 years.

While the comparison to the reference reactor inventory does not ideally verify the model, the fact remains that burning the standard amount of fuel for a standard fuel residency time has MCNP correctly calculate accurate burnup values as discussed in the previous section, and this should add credibility to the MCNP models.

4.3.2 The Isotopes of Interest

Using the ratio values calculated in Tables 4.6 and 4.7, the original thesis problem of why these specific isotopes are of interest to decommissioning to the regulatory body of one country and not the other. Combining these ratio values from Tables 4.6 and 4.7 with the data in Table 2.2, Table 4.9 is generated to address this question.

Table 4.9:

Comparison of the Isotopic Concentrations of the Isotopes of Interest

Isotope	Ratio of FUGEN over Pickering	Of interest to Canada	Of interest to Japan
Mo-93	N/A	No	Yes
Ag-107	8.8	No	Yes
Cs-134	43.1	No	Yes
Ho-165	2.9	No	Yes
Am-243	Infinite	No	Yes
Sn-120	1.5	Yes	No

Note. The Table shows the ratio of isotopic densities of the isotopes of interests and whether that isotope is considered as of interest to Canada or Japan. The ^{243}Am is considered as appearing infinitely more as none is generated in the Pickering fuel. The ^{93}Mo is shown as N/A as none is generated in the Pickering reactor and the amounts generated in the FUGEN model are not in the fuel.

From Table 4.9, it can be seen that, the majority of the isotopes of interest to Japan appear in higher concentrations in the FUGEN model than in the Pickering model. With the earlier assumption that the reasons for why these isotopes of interest are entirely radiological, the results shown in Table 4.9 show a valid explanation as to why they are of interest. This is except for the ^{120}Sn, which should be of interest to Canada and not Japan. The comparison shows that the ^{120}Sn is still more concentrated in the FUGEN model than in the Pickering model. It is possible, however, that there are nonradioactive reasons for why these elements are of interest to one country and not the other, such as toxicity, as well as that it is ^{121m}Sn which is of interest, not ^{120}Sn.

Chapter 5

Conclusions

The purpose of this thesis has been to develop MCNP models of the Pickering and FUGEN reactors in order to examine their radioactive inventories and come to an understanding of why the chosen list of isotopes were determined as being of interest to only one of the countries which regulate these reactors. Through this examination and comparison of these isotopes, the reasons for which one country may consider these specific isotopes to be of concern while the other does not are better understood.

A background on the FUGEN and Pickering reactors as well as MCNP was given in order to give an understanding of the production of the models as well as the comparisons which are made throughout the thesis. Dimensional data on the reactors was found from several pieces of literature and was used to produce MCNP models of the fuel assemblies used in the reactors. These MCNP models then underwent depletion calculations in order to burn the fuels for their expected fuel residency times. From these fuel depletion tests, lists of isotopes created through both fission and neutron activation were produced. These depletion tests also calculated the

burnup values the fuel had undergone, which was compared to reference values for the verification of the models. Examination of the isotopes of interest on a per-volume basis did show possible indication of why the regulatory bodies of one country would find a specific isotope to be of concern while the other does not.

Comparisons of the models to reference data at times showed acceptable correlation, while certain isotopes were shown to vary greatly. The MCNP models generated through the thesis only represent a very small part of the reactor and may differ from reference models, which are based on entire reactors. However, when compared to each other, they should give a reasonable understanding of the difference inherent between these reactors, which arise from their many design differences.

5.1 Further Work

The models produced through this thesis only represent a tiny part of the reactors in question. A larger model more accurately representing the reactor core in its entirety would significantly improve the accuracy and usefulness of the MCNP models. This would entail a relatively large undertaking, including the modelling of various seals, valves and plugs which are present within the reactor and can be made of a variety of polymers and alloys, which could be activated and greatly alter the inventory of the reactors after decades of operation.

Another focus on further work to improve these models would be to increase the understanding of the reactor materials as well as the fuel parameters under which the reactor runs. The creation of the models is based on data coming mainly from scientific articles and technical reports, but these do not give a thorough understanding of the conditions in which the reactors were built and operated for decades. An example of

the difference this greater understanding of the materials would create is in learning of the presence of impurities. An isotopic breakdown of the reactor's materials coming from a mass spectrometer could give an in-depth view of the impurities within the reactor which could possibly explain the presence of unexpected isotopes through neutron activation.

Future work could also focus on mapping out the areas of higher reactivity within the reactors themselves. For the purposes of these models, averages are used for enrichment and neutron activation. In a more realistic model, there will be areas within the reactor that undergo differing levels of reactivity, with those closest to the centre of the reactor being under more stress. In reality, the FUGEN reactor utilized several different types of fuel layout with differing amounts of enrichment which were simplified to an average for this project. In order to make a more realistic model, these differing fuel layouts could be modelled, more accurately depicting the areas of higher and lower activity within the reactor core.

Additional future work to better the work done in this thesis would be for MCNP's built in fractional standard deviation to be calculated for criticality calculations. As it currently stands, MCNP does not calculate the FSD for criticality calculations. This greatly affects the results of the research as there is no way to know how large the range of values associated with the calculated inventories is.

References

Agency for Toxic Substances and Disease Registry (ATSDR). (2004). *Toxicological profile for cesium* (Tech. Rep.). Atlanta, GA.

Agency for Toxic Substances and Disease Registry (ATSDR). (2005). *Toxicological profile for tin and tin compounds* (Tech. Rep.). Atlanta, GA.

Application of the concepts of exclusion, exemption and clearance (No. RS-G-1.7). (2004). Vienna: International Atomic Energy Agency. Retrieved from `https://www-pub.iaea.org/MTCD/Publications/PDF/Pub1202_web.pdf`

Barber, D. H. (2013). Implementation of a thermodynamic solver within a computer program for calculating fission-product release fractions. *Ph.D. dissertation, Royal Military College of Canada.*

Barber, D. H. (2014, June). Benchmarking nuclide computations in nuclear safety analysis computer programs,. In *Proceedings of the phwr safety 2014/cansas-2014 workshop.* Ottawa, On.

Bomboni, E., Cerullo, N., Fridman, E., Lomonaco, G., & Shwageraus, E. (2010). Comparison among MCNP-based depletion codes applied to burnup calculations of pebble-bed HTR lattices. *Nuclear Engineering and Design*, *240*(4), 918–924.

Brooks, G. L. (1993). *A short history of the CANDU nuclear power system* (Tech. Rep.). Atomic Energy of Canada Ltd., AECL–10788.

Bryan, J. C. (2018). *Introduction to nuclear science* (2nd ed.). Boca Raton, FL. United States: CRC press.

Canadian Nuclear Safety Commission. (2018, January 23). Technical Update on Fuel Channel Fitness-For-Service in Canadian Nuclear Power Plants [PowerPoint slides], CMD 18-M4.

Canadian Nuclear Safety Commission. (2021, Mar). REGDOC-2.9.2 Controlling Releases to the Environment [Draft]. Retrieved from http://nuclearsafety.gc.ca/eng/acts-and-regulations/regulatory-documents/index.cfm

Cember, H., & Johnson, T. E. (2008). *Introduction to health physics*. McGraw-Hill Companies, Inc.

Cho, D., Sun, G., Choi, J., Yang, H., & Hwang, T. (2011). Verification of source term estimation method against measured data for decommissioning waste from a CANDU reactor. *Journal of nuclear science and technology*, *48*(7), 1087–1093.

Classification of radioactive waste (No. GSG-1). (2009). Vienna: International Atomic Energy Agency. Retrieved from https://www.iaea.org/publications/8154/classification-of-radioactive-waste

Department of Justice Canada. (2000). *Nuclear substances and radiation devices regulations sor/2000-207.* Available at https://laws-lois.justice.gc.ca/eng/regulations/sor-2000-207/FullText.html.

Eckerman, K., & Endo, A. (2008). ICRP Publication 107. Nuclear decay data for dosimetric calculations. *Annals of the ICRP*, *38*(3), 7.

Fensin, M. L. (2008). *Development of the MCNPX depletion capability: A Monte Carlo linked depletion method that automates the coupling between MCNPX and CINDER90 for high fidelity burnup calculations* (Unpublished doctoral dissertation). Gainesville, FL, United States.

Fensin, M. L., James, M. R., Hendricks, J. S., & Goorley, J. T. (2011). The new MCNP6 depletion capability. *LA-UR 11-07032*.

Fission product yield. (2008). In Wikipedia, Retrieved 2022, March 10. Retrieved from https://en.wikipedia.org/wiki/Fission_product_yield

FUGEN Decommissioning Engineering Center. (2015, May 25). History of Fugen. Retrieved from https://www.jaea.go.jp/04/fugen/en/guide/history/

Gilbert, J. (2016). *Simulation of In-Core Dose Rates for an Offline CANDU Reactor* (Unpublished master's thesis). University of Ontario Institute of Technology.

Girard, S., Little, R., White, M., Lee, M., & Trellue, H. (2003). MCNP A General Monte Carlo N-Particle Transport Code, Version 5. *LA-UR-03-1987*, *1*.

Harvel, G. (2019, May 6). Lecture LM1B: Concepts of Decommissioning [PowerPoint slides]. University of Ontario Institute of Technology, Special Topics: Decommissioning Canvas. Retrieved from learn.ontariotechu.ca

Hastings, I. (1982). *Structures in irradiated U02 from Canadian reactors* (Tech. Rep.). Atomic Energy of Canada Limited Report, AECL-MISC-249.

Hattori, T. (2020). Trend of strengthening clearance regulation in Japan and concerns about its worldwide effects on regulations for natural and artificial radionuclides. *Annals of the ICRP*, *49*(1_suppl), 98–112.

Henderson, D., Anderson, M., Thomas, D., & Benton, H. (1997). *MCNP CRC Reactivity Calculation For Quad Cities BWR* (Tech. Rep.). Civilian Radioactive Waste Management System Management & Operating Contractor, 1300000000-01717 0200o00146 REV 00.

Hou, X. (2005). Radiochemical determination of 41Ca in nuclear reactor concrete. *Radiochimica Acta*, *93*(9-10), 611-617.

Hussein, E. (2016). Monte Carlo Particle transport with MCNP, Chapter 11 - Uncertainty analysis in MCNP [PowerPoint slides]. University of New Brunswick, Department of Mechanical Engineering. Retrieved from https://canteach.candu.org/Content%20Library/20043524.pdf

Ikusawa, Y., Kikuchi, K., & Ozawa, T. (2005). *Post Irradiation Examination for the FUGEN High Burn-up MOX Fuel Assembly (III)* (Tech. Rep.). Japan Nuclear Cycle Development Institute, JNC TN8410 2005-012, Ibaraki, Japan.

International Atomic Energy Agency. (1994). *Advances in heavy water reactors (proceedings of a technical committee meeting, toronto, 7-10 june 1993).* Vienna: IAEA TECDOC No. 738.

International Atomic Energy Agency. (1998). *Water channel reactor fuels and fuel channels: Design, performance, research and development.* Vienna: IAEA TECDOC No. 997.

International Commission on Radiological Protection. (2017). Occupational intakes of radionuclides: part 3. ICRP publication 137. *Ann. ICRP*, *46*, 3-4.

Kato, H., & Miyawaki, Y. (1976). Nuclear design and its development for FUGEN. United States.

Kerlin, T. W., & Upadhyaya, B. R. (2019). *Dynamics and control of nuclear reactors.* Elsevier Science & Technology.

Knoll, G. F. (2010). *Radiation detection and measurement* (4th ed.). Ann Arbor, Michigan, United States: John Wiley & Sons.

Love, E., Pauley, K., & Reid, B. (1995). *Use of MCNP for characterization of reactor vessel internals waste from decommissioned nuclear reactors* (Tech. Rep.). INEL-95/0419, (United States). doi: https://doi.org/10.2172/130639

MatWeb: Online Materials Information Resource. (n.d.). *Zr-2.5Nb Zirconium Alloy, Nuclear Grade.* Available at `https://www.matweb.com/search/datasheet_print.aspx?matguid=9c996807673f4208bc99c655c388072d` Retrieved 2022, March 10.

Mehta, K. (1982). *Nuclide inventory for nuclear fuel waste management: Post-closure phase* (Tech. Rep.). Atomic Energy of Canada Limited Report, AECL-6830.

Micklich, B. J. (2015, April 15-17). CINDER2008 - A New Version of CINDER [PowerPoint slides]. In *3rd international workshop on accelerator radiation induced activation ARIA 2015.* Knoxville TN, USA. Retrieved from https://public.ornl.gov/neutrons/conf/aria2015/presentations/09%20CINDER2008-%20A%20New%20Version%20of%20CINDER.pdf

Ministry of the Environment, Government of Japan. (2018). *Booklet to provide basic information regarding health effects of radiation (1st edition), chapter 2.2 - radiation exposure.* Available at https://www.env.go.jp/en/chemi/rhm/basic-info/1st/pdf/basic-1st-02-02-04.pdf Retrieved 2022, March 10.

Ohtani, T., Iijima, T., & Shiratori, Y. (2003). Analysis of mixed oxide fuel loaded cores in the heavy water reactor FUGEN. *Journal of nuclear science and technology*, *40*(11), 959-969. doi: https://doi.org/10.1080/18811248.2003.9715439

Organisation for Economic Co-operation and Development and Nuclear Energy Agency. (2006). *Strategy selection for the decommissioning of nuclear facilities, isbn 92-64-02305-4.* Paris. OECD Publishing.

Paquet, F., Bailey, M., Leggett, R., Etherington, G., Blanchardon, E., Smith, T., ... others (2019). ICRP Publication 141: Occupational Intakes of Radionuclides: Part 4. *Annals of the ICRP*, *48*(2-3), 9-501.

Paquet, F., Bailey, M., Leggett, R., Lipsztein, J., Fell, T., Smith, T., ... others (2016). ICRP Publication 134: Occupational intakes of radionuclides: Part 2. *Annals of the ICRP*, *45*(3-4), 7–349.

Phalen, R. F., Morrow, P. E., Raabe, O., & Velasquez, D. (1973). Experimental inhalation of metallic silver. *Health physics, Volume 24*.

Popov, N. K. (2014). Thermal-hydraulic design. In W. J. Garland (Ed.), *The essential candu* (chap. 6). Hamilton: University Network of Excellence in Nuclear Engineering.

Rouben, B. (1999). CANDU Fuel Management Course. *Atomic Energy of Canada Ltd.* Retrieved from https://canteach.candu.org/content%20library/20031101.pdf

Sawai, S., Haga, T., Akebi, M., & Kontani, K. (1979). Fugen hwr reaches commercial operation. *Nuclear Engineering International*, *24*(289), 33-44.

Shiratori, Y., Furubayashi, T., & Matsumoto, M. (1993). Operating experience with mox fuel loaded heavy water reactor. *Journal of Nuclear Science and Technology*, *30*(1), 78-88. doi: https://doi.org/10.1080/18811248.1993.9734451

Shultis, J. K., & Faw, R. E. (2000). *Radiation shielding.* Inc., La Grange Park, IL, Unites States: American Nuclear Society.

Sowby, F. (1983). Radionuclide transformations - energy and intensity of emissions. *Annals of the ICRP*, *38*, 11-13.

Tanaka, K., Maeda, K., Sasaki, S., Ikusawa, Y., & Abe, T. (2006). Fuel–cladding chemical interaction in MOX fuel rods irradiated to high burnup in an advanced thermal reactor. *Journal of nuclear materials*, *357*(1-3), 58–68.

Tezuka, M., Koda, Y., Iguchi, Y., Kato, Y., & Yanagihara, S. (2017, Feb 7-9). *Lessons-learned from ongoing decommissioning project of Fugen NPS [PowerPoint slides].* Research Institute of Nuclear Engineering, University of Fukui. Retrieved from https://inis.iaea.org/collection/NCLCollectionStore/_Public/48/047/48047389.pdf

The Engineering ToolBox. (2017). *Heavy Water - Thermophysical Properties.* Available at www.engineeringtoolbox.com/heavy-water-thermodynamic-properties-d_2003.html Retrieved 2022, March 10.

Trellue, H., Poston, D., & User's Manual, V. (1999). *2.0 for monteburns* (Tech. Rep.). Version 1.0, Tech. Rep. LA-UR-99-4999, LANL (September 1999).

United States Nuclear Regulatory Commission. (2018). *Backgrounder on high burnup spent nuclear fuel.* Available at `https://www.nrc.gov/docs/ML1827/ML18270A110.pdf` Retrieved 2022, March 11.

Wasywich, K. (1993). *Characteristics of used CANDU fuel relevant to the Canadian nuclear fuel waste management program* (Tech. Rep.). Atomic Energy of Canada Ltd.,AECL-10463, COG-91-340.

Werner, C. J., et al. (2017). MCNP Users Manual-Code Version 6.2. *Los Alamos National Laboratory, LA-UR-17-29981*.

Williams, R. G., Gesh, C. J., & Pagh, R. T. (2006). *Compendium of material composition data for radiation transport modeling* (Tech. Rep.). Pacific Northwest National Lab.(PNNL), Richland, WA (United States).

Yan, H., Bromley, B. P., Dugal, C., & Colton, A. V. (2018). Modeling studies and code-to-code comparisons for pressure tube heavy water reactor cores. *CNL Nuclear Review*, *7*(2), 177–200.

Appendix A - Pickering MCNP Input Code

```
Pickering A 28-Element Fuel Bundle 1-year
c ======== Cell Card ==========
100 1 -10.6   -1001          imp:n=1 vol=76.6602 u=1 $ Pellet/
   Stick
101 4 -1.7     1001 -1002    imp:n=1 vol=0.2184 u=1 $ CANLUB
102 2 -6.56    1002 -1003    imp:n=1 vol=8.7668 u=1 $ Zirc4
   Sheath
103 3 -1.11    1003          imp:n=1 u=1
104 3 -1.11   -1004          imp:n=1 lat=1 u=2 fill=0:0 0:3 0:3
                 1 1 1 1
                 1 1 1 1
                 1 1 1 1
                 1 1 1 1
105 0         -1005          imp:n=1 fill=2
106 3 -1.11    1005 1012 1015 1018 1021 1024 1027 1030 1033
   1036 1039 &
        1042 1045 -1006 imp:n=1 vol=3311.9769 $Pressure tube
           water
```

```
107 5 -6.56    1006 -1007    imp:n=1 vol=3363.5016 $ Pressure
   tube
108 0          1007          imp:n=0 $ Outside Universe
c ======== More Fuel Pins ==========
110 1 -10.6   -1010          imp:n=1 vol=76.6602 $ Top left
111 4 -1.7     1010 -1011    imp:n=1 vol=0.2184 $ Top left
112 2 -6.56    1011 -1012    imp:n=1 vol=8.7668 $ Top left
113 1 -10.6   -1013          imp:n=1 vol=76.6602 $ Top middle
114 4 -1.7     1013 -1014    imp:n=1 vol=0.2184 $ Top middle
115 2 -6.56    1014 -1015    imp:n=1 vol=8.7668 $ Top middle
116 1 -10.6   -1016          imp:n=1 vol=76.6602 $ Top right
117 4 -1.7     1016 -1017    imp:n=1 vol=0.2184 $ Top right
118 2 -6.56    1017 -1018    imp:n=1 vol=8.7668 $ Top right
119 1 -10.6   -1019          imp:n=1 vol=76.6602 $ Right top
120 4 -1.7     1019 -1020    imp:n=1 vol=0.2184 $ Right top
121 2 -6.56    1020 -1021    imp:n=1 vol=8.7668 $ Right top
122 1 -10.6   -1022          imp:n=1 vol=76.6602 $ Right middle
123 4 -1.7     1022 -1023    imp:n=1 vol=0.2184 $ Right middle
124 2 -6.56    1023 -1024    imp:n=1 vol=8.7668 $ Right middle
125 1 -10.6   -1025          imp:n=1 vol=76.6602 $ Right bottom
126 4 -1.7     1025 -1026    imp:n=1 vol=0.2184 $ Right bottom
127 2 -6.56    1026 -1027    imp:n=1 vol=8.7668 $ Right bottom
128 1 -10.6   -1028          imp:n=1 vol=76.6602 $ Bottom left
129 4 -1.7     1028 -1029    imp:n=1 vol=0.2184 $ Bottom left
130 2 -6.56    1029 -1030    imp:n=1 vol=8.7668 $ Bottom left
131 1 -10.6   -1031          imp:n=1 vol=76.6602 $ Bottom middle
132 4 -1.7     1031 -1032    imp:n=1 vol=0.2184 $ Bottom middle
```

```
133 2 -6.56   1032 -1033  imp:n=1 vol=8.7668 $ Bottom middle
134 1 -10.6   -1034       imp:n=1 vol=76.6602 $ Bottom right
135 4 -1.7    1034 -1035  imp:n=1 vol=0.2184 $ Bottom right
136 2 -6.56   1035 -1036  imp:n=1 vol=8.7668 $ Bottom right
137 1 -10.6   -1037       imp:n=1 vol=76.6602 $ Left top
138 4 -1.7    1037 -1038  imp:n=1 vol=0.2184 $ Left top
139 2 -6.56   1038 -1039  imp:n=1 vol=8.7668 $ Left top
140 1 -10.6   -1040       imp:n=1 vol=76.6602 $ Left middle
141 4 -1.7    1040 -1041  imp:n=1 vol=0.2184 $ Left middle
142 2 -6.56   1041 -1042  imp:n=1 vol=8.7668 $ Left middle
143 1 -10.6   -1043       imp:n=1 vol=76.6602 $ Left bottom
144 4 -1.7    1043 -1044  imp:n=1 vol=0.2184 $ Left bottom
145 2 -6.56   1044 -1045  imp:n=1 vol=8.7668 $ Left bottom

c ======== Surface Card ==========
1001 rcc 0.04 0 0 48 0 0 0.713          $ Pellet (L=480mm) d
   =14.26mm
1002 rcc 0.039 0 0 48.002 0 0 0.714  $ Canlub (L=480.02mm) t
   =0.01mm
1003 rcc 0 0 0 48.08 0 0 0.753          $ Cladding (L=480.78mm)
    t=0.39mm
1004 box -0.1 -0.78 -0.78 48.20 0 0 0 1.56 0 0 0 1.56
   $Imaginary box
1005 box -0.1 -0.78 -0.78 48.20 0 0 0 6.24 0 0 0 6.24
   $Lattice bounds
1006 rcc -10 2.34 2.34 68 0 0 5.17     $ Inner pressure tube (
   d=103.4mm)
```

```
1007 rcc -10 2.34 2.34 68 0 0 5.59     $ Outer pressure tube
   (4.2mm thick)
c ======== More Fuel Pins ==========
1010 rcc 0.04 0.78 6.24 48 0 0 0.713        $ Top left
1011 rcc 0.039 0.78 6.24 48.002 0 0 0.714   $ Top left
1012 rcc 0 0.78 6.24 48.08 0 0 0.753        $ Top left
1013 rcc 0.04 2.34 6.24 48 0 0 0.713        $ Top middle
1014 rcc 0.039 2.34 6.24 48.002 0 0 0.714   $ Top middle
1015 rcc 0 2.34 6.24 48.08 0 0 0.753        $ Top middle
1016 rcc 0.04 3.9 6.24 48 0 0 0.713         $ Top right
1017 rcc 0.039 3.9 6.24 48.002 0 0 0.714    $ Top right
1018 rcc 0 3.9 6.24 48.08 0 0 0.753         $ Top right
1019 rcc 0.04 6.24 3.9 48 0 0 0.713         $ Right top
1020 rcc 0.039 6.24 3.9 48.002 0 0 0.714    $ Right top
1021 rcc 0 6.24 3.9 48.08 0 0 0.753         $ Right top
1022 rcc 0.04 6.24 2.34 48 0 0 0.713        $ Right middle
1023 rcc 0.039 6.24 2.34 48.002 0 0 0.714   $ Right middle
1024 rcc 0 6.24 2.34 48.08 0 0 0.753        $ Right middle
1025 rcc 0.04 6.24 0.78 48 0 0 0.713        $ Right bottom
1026 rcc 0.039 6.24 0.78 48.002 0 0 0.714   $ Right bottom
1027 rcc 0 6.24 0.78 48.08 0 0 0.753        $ Right bottom
1028 rcc 0.04 0.78 -1.56 48 0 0 0.713       $ Bottom left
1029 rcc 0.039 0.78 -1.56 48.002 0 0 0.714  $ Bottom left
1030 rcc 0 0.78 -1.56 48.08 0 0 0.753       $ Bottom left
1031 rcc 0.04 2.34 -1.56 48 0 0 0.713       $ Bottom middle
1032 rcc 0.039 2.34 -1.56 48.002 0 0 0.714  $ Bottom middle
1033 rcc 0 2.34 -1.56 48.08 0 0 0.753       $ Bottom middle
```

```
1034 rcc 0.04 3.9 -1.56 48 0 0 0.713        $ Bottom right
1035 rcc 0.039 3.9 -1.56 48.002 0 0 0.714    $ Bottom right
1036 rcc 0 3.9 -1.56 48.08 0 0 0.753         $ Bottom right
1037 rcc 0.04 -1.56 3.9 48 0 0 0.713         $ Left top
1038 rcc 0.039 -1.56 3.9 48.002 0 0 0.714    $ Left top
1039 rcc 0 -1.56 3.9 48.08 0 0 0.753         $ Left top
1040 rcc 0.04 -1.56 2.34 48 0 0 0.713        $ Left middle
1041 rcc 0.039 -1.56 2.34 48.002 0 0 0.714   $ Left middle
1042 rcc 0 -1.56 2.34 48.08 0 0 0.753        $ Left middle
1043 rcc 0.04 -1.56 0.78 48 0 0 0.713        $ Left bottom
1044 rcc 0.039 -1.56 0.78 48.002 0 0 0.714   $ Left bottom
1045 rcc 0 -1.56 0.78 48.08 0 0 0.753        $ Left bottom

c ========= Data Card ==========
MPHYS ON
ACT DN=MODEL
KCODE 10000 1.0 50 150 $ BURN Parameters
KSRC 24 0.78 6.24 24 2.34 6.24 24 3.9 6.24 24 6.24 3.9 24
   6.24 2.34 &
        24 6.24 0.78 24 3.9 -1.56 24 2.34 -1.56 24 0.78 -1.56
            24 -1.56 0.78 &
        24 -1.56 2.34 24 -1.56 3.9 24 0 4.68 24 1.56 4.68 24
           3.12 4.68 &
        24 4.68 4.68 24 0 3.12 24 1.56 3.12 24 3.12 3.12 24
           4.68 3.12 &
        24 0 1.56 24 1.56 1.56 24 3.12 1.56 24 4.68 1.68 24 0
            0 24 1.68 0 &
```

```
          24  3.12  0  24  4.68  0
c ========= BURN Parameters ==========
BURN Time=320 PFRAC=1 POWER=0.426666666666667 MAT=1 2 BOPT
    =1.0  24  1 &
          MATVOL=2146.49  245.47
c ========= Material Card ==========
m1   92234 -0.0000468 92235 -0.00627 92238 -0.875 &
          8016 -0.118 8017 -0.0000479 $NUO2
m2   24050 -0.004 24052 -0.084 24053 -0.010 24054 -0.002 &
          26054 -0.011 26056 -0.184 26057 -0.004 26058 -0.001 &
          8016 -0.12 40000 -98.180 50000 -1.4 $ Zirc4
m3   1001 -0.00028 1002 -0.1995 8016 -0.80022 $ Heavy water
mt3 hwtr
m4   6000 -0.999999 $ Reactor grade graphite
m5   24050 -0.004 24052 -0.084 24053 -0.010 24054 -0.002 &
          26054 -0.011 26056 -0.184 26057 -0.004 26058 -0.001 &
          8016 -0.12 40000 -98.181 50000 -1.4 $ Zirc4
print
```

Appendix B - FUGEN MCNP Input Code

```
FUGEN Standard MOX Fuel Assembly (28 Rod Driver)
c ========= Cell Card ==========
100 1 -10.27 -1001          imp:n=1 vol=602.5826 u=1 $ Pellet/
   Stick
101 2 -6.56   1001 -1002  imp:n=1 vol=160.4320 u=1 $ Zirc2
   Sheath
102 3 -1       1002         imp:n=1 u=1 $ Water box
103 0         -1003         imp:n=1 lat=1 u=2 fill=0:1 0:5 0:0
         1 1
         1 1
         1 1
         1 1
         1 1
         1 1
104 0         -1004         imp:n=1 fill=2
105 3 -1       1004 1011 1013 1015 1017 1019 1021 1023 1025
   1027 &
```

```
        1029 1031 1033 1035 1037 1039 1041 1043 1045 1047
           1049 1050 &
        1051 1052 1053 1054 1055 1056 1057 1058 1059 1060
           1061 -1005 &
        imp:n=1 vol=21141.0847 $ Pressure tube water
106 4 -6.44    1005 -1006  imp:n=1 vol=6432.7785 $ Pressure
   tube
107 0          1006        imp:n=0 $ Outside universe
c ======== More Fuel Pins ==========
110 1 -10.27   -1010        imp:n=1 vol=602.5826 $ Top Left
111 2 -6.56     1010 -1011  imp:n=1 vol=160.4320 $ Top Left
112 1 -10.27   -1012        imp:n=1 vol=602.5826 $ Top Right
113 2 -6.56     1012 -1013  imp:n=1 vol=160.4320 $ Top Right
114 1 -10.27   -1014        imp:n=1 vol=602.5826 $ Bottom Left
115 2 -6.56     1014 -1015  imp:n=1 vol=160.4320 $ Bottom Left
116 1 -10.27   -1016        imp:n=1 vol=602.5826 $ Bottom
   Right
117 2 -6.56     1016 -1017  imp:n=1 vol=160.4320 $ Bottom
   Right
118 1 -10.27   -1018        imp:n=1 vol=602.5826 $ Far left
   top
119 2 -6.56     1018 -1019  imp:n=1 vol=160.4320 $ Far left
   top
120 1 -10.27   -1020        imp:n=1 vol=602.5826 $ Far left
   bottom
121 2 -6.56     1020 -1021  imp:n=1 vol=160.4320 $ Far left
   bottom
```

```
122 1 -10.27  -1022        imp:n=1 vol=602.5826 $ Far right
   top
123 2 -6.56    1022 -1023  imp:n=1 vol=160.4320 $ Far right
   top
124 1 -10.27  -1024        imp:n=1 vol=602.5826 $ Far right
   bottom
125 2 -6.56    1024 -1025  imp:n=1 vol=160.4320 $ Far right
   bottom
126 1 -10.27  -1026        imp:n=1 vol=602.5826 $ Far left
   middle upper
127 2 -6.56    1026 -1027  imp:n=1 vol=160.4320 $ Far left
   middle upper
128 1 -10.27  -1028        imp:n=1 vol=602.5826 $ Far left
   middle lower
129 2 -6.56    1028 -1029  imp:n=1 vol=160.4320 $ Far left
   middle lower
130 1 -10.27  -1030        imp:n=1 vol=602.5826 $ Left middle
    upper
131 2 -6.56    1030 -1031  imp:n=1 vol=160.4320 $ Left middle
    upper
132 1 -10.27  -1032        imp:n=1 vol=602.5826 $ Left middle
    lower
133 2 -6.56    1032 -1033  imp:n=1 vol=160.4320 $ Left middle
    lower
134 1 -10.27  -1034        imp:n=1 vol=602.5826 $ Far right
   middle upper
```

```
135 2 -6.56    1034 -1035  imp:n=1 vol=160.4320 $ Far right
   middle upper
136 1 -10.27  -1036        imp:n=1 vol=602.5826 $ Far right
   middle lower
137 2 -6.56    1036 -1037  imp:n=1 vol=160.4320 $ Far right
   middle lower
138 1 -10.27  -1038        imp:n=1 vol=602.5826 $ Right
   middle upper
139 2 -6.56    1038 -1039  imp:n=1 vol=160.4320 $ Right
   middle upper
140 1 -10.27  -1040        imp:n=1 vol=602.5826 $ Right
   middle lower
141 2 -6.56    1040 -1041  imp:n=1 vol=160.4320 $ Right
   middle lower
c ======== Tie rods ==========
142 3 -1      -1042        imp:n=1 vol=91.1757 $ Top Left Tie
   Rod
143 2 -6.56   1042 -1043  imp:n=1 vol=51.2863 $ Top Left Tie
   Rod
144 3 -1      -1044        imp:n=1 vol=91.1757 $ Top Right Tie
    Rod
145 2 -6.56   1044 -1045  imp:n=1 vol=51.2863 $ Top Right Tie
    Rod
146 3 -1      -1046        imp:n=1 vol=91.1757 $ Bottom Left
   Tie Rod
147 2 -6.56   1046 -1047  imp:n=1 vol=51.2863 $ Bottom Left
   Tie Rod
```

```
148 3 -1      -1048          imp:n=1 vol=91.1757 $ Bottom Right
   Tie Rod
149 2 -6.56    1048 -1049   imp:n=1 vol=51.2863 $ Bottom Right
   Tie Rod
c ======== Spacers ==========
150 5 -8.19    1004 1011 1013 1015 1017 1019 1021 1023 1025
   1027 1029 1031 &
         1033 1035 1037 1039 1041 1043 1045 1047 1049 -1050
            imp:n=1 vol=92.86
151 5 -8.19    1004 1011 1013 1015 1017 1019 1021 1023 1025
   1027 1029 1031 &
         1033 1035 1037 1039 1041 1043 1045 1047 1049 -1051
            imp:n=1 vol=92.86
152 5 -8.19    1004 1011 1013 1015 1017 1019 1021 1023 1025
   1027 1029 1031 &
         1033 1035 1037 1039 1041 1043 1045 1047 1049 -1052
            imp:n=1 vol=92.86
153 5 -8.19    1004 1011 1013 1015 1017 1019 1021 1023 1025
   1027 1029 1031 &
         1033 1035 1037 1039 1041 1043 1045 1047 1049 -1053
            imp:n=1 vol=92.86
154 5 -8.19    1004 1011 1013 1015 1017 1019 1021 1023 1025
   1027 1029 1031 &
         1033 1035 1037 1039 1041 1043 1045 1047 1049 -1054
            imp:n=1 vol=92.86
155 5 -8.19    1004 1011 1013 1015 1017 1019 1021 1023 1025
   1027 1029 1031 &
```

```
        1033 1035 1037 1039 1041 1043 1045 1047 1049 -1055
           imp:n=1 vol=92.86
156 5 -8.19   1004 1011 1013 1015 1017 1019 1021 1023 1025
   1027 1029 1031 &
        1033 1035 1037 1039 1041 1043 1045 1047 1049 -1056
           imp:n=1 vol=92.86
157 5 -8.19   1004 1011 1013 1015 1017 1019 1021 1023 1025
   1027 1029 1031 &
        1033 1035 1037 1039 1041 1043 1045 1047 1049 -1057
           imp:n=1 vol=92.86
158 5 -8.19   1004 1011 1013 1015 1017 1019 1021 1023 1025
   1027 1029 1031 &
        1033 1035 1037 1039 1041 1043 1045 1047 1049 -1058
           imp:n=1 vol=92.86
159 5 -8.19   1004 1011 1013 1015 1017 1019 1021 1023 1025
   1027 1029 1031 &
        1033 1035 1037 1039 1041 1043 1045 1047 1049 -1059
           imp:n=1 vol=92.86
160 5 -8.19   1004 1011 1013 1015 1017 1019 1021 1023 1025
   1027 1029 1031 &
        1033 1035 1037 1039 1041 1043 1045 1047 1049 -1060
           imp:n=1 vol=92.86
161 5 -8.19   1004 1011 1013 1015 1017 1019 1021 1023 1025
   1027 1029 1031 &
        1033 1035 1037 1039 1041 1043 1045 1047 1049 -1061
           imp:n=1 vol=92.86
```

```
c ======== Surface Card ==========
1001 rcc 0 0 0.09 0 0 370 0.72 $ Pellet/Rod (L=3700mm) Meat
   =3.7m
1002 rcc 0 0 0 0 0 370.18 0.81 $ Cladding (L=3701.8mm)
   Cladding t=0.9mm
1003 box -0.84 -0.84 -0.1 1.68 0 0 0 1.68 0 0 0 370.4
   $Imaginary box
1004 box -0.84 -0.84 -0.1 3.36 0 0 0 10.08 0 0 0 370.4
   $Lattice
1005 rcc 0.84 4.2 -10 0 0 390 5.89 $ Inner pressure tube wall
    (r=58.9mm)
1006 rcc 0.84 4.2 -10 0 0 390 6.32 $ Outer pressure tube wall
    (r=63.2mm)
c ======== More Fuel Pins ==========
1010 rcc -1.68 8.4 0.09 0 0 370 0.72 $ Top left
1011 rcc -1.68 8.4 0 0 0 370.18 0.81 $ Top left
1012 rcc  3.36 8.4 0.09 0 0 370 0.72 $ Top Right
1013 rcc  3.36 8.4 0 0 0 370.18 0.81 $ Top Right
1014 rcc -1.68 0 0.09 0 0 370 0.72 $ Bottom left
1015 rcc -1.68 0 0 0 0 370.18 0.81 $ Bottom left
1016 rcc  3.36 0 0.09 0 0 370 0.72 $ Bottom Right
1017 rcc  3.36 0 0 0 0 370.18 0.81 $ Bottom Right
1018 rcc -3.36 6.72 0.09 0 0 370 0.72 $ Far left top
1019 rcc -3.36 6.72 0 0 0 370.18 0.81 $ Far left top
1020 rcc -3.36 1.68 0.09 0 0 370 0.72 $ Far left bottom
1021 rcc -3.36 1.68 0 0 0 370.18 0.81 $ Far left bottom
1022 rcc  5.04 6.72 0.09 0 0 370 0.72 $ Far right top
```

```
1023 rcc  5.04 6.72 0 0 0 370.18 0.81 $ Far right top
1024 rcc  5.04 1.68 0.09 0 0 370 0.72 $ Far right bottom
1025 rcc  5.04 1.68 0 0 0 370.18 0.81 $ Far right bottom
1026 rcc -3.36 5.04 0.09 0 0 370 0.72 $ Far left middle upper
1027 rcc -3.36 5.04 0 0 0 370.18 0.81 $ Far left middle upper
1028 rcc -3.36 3.36 0.09 0 0 370 0.72 $ Far left middle lower
1029 rcc -3.36 3.36 0 0 0 370.18 0.81 $ Far left middle lower
1030 rcc -1.68 5.04 0.09 0 0 370 0.72 $ Left middle upper
1031 rcc -1.68 5.04 0 0 0 370.18 0.81 $ Left middle upper
1032 rcc -1.68 3.36 0.09 0 0 370 0.72 $ Left middle lower
1033 rcc -1.68 3.36 0 0 0 370.18 0.81 $ Left middle lower
1034 rcc  5.04 5.04 0.09 0 0 370 0.72 $ Far right middle
   upper
1035 rcc  5.04 5.04 0 0 0 370.18 0.81 $ Far right middle
   upper
1036 rcc  5.04 3.36 0.09 0 0 370 0.72 $ Far right middle
   lower
1037 rcc  5.04 3.36 0 0 0 370.18 0.81 $ Far right middle
   lower
1038 rcc  3.36 5.04 0.09 0 0 370 0.72 $ Right middle upper
1039 rcc  3.36 5.04 0 0 0 370.18 0.81 $ Right middle upper
1040 rcc  3.36 3.36 0.09 0 0 370 0.72 $ Right middle lower
1041 rcc  3.36 3.36 0 0 0 370.18 0.81 $ Right middle lower
c ======== Tie rods ==========
1042 rcc -1.68 6.72 0 0 0 370.18 0.28 $ Top Left Tie Rod
1043 rcc -1.68 6.72 0 0 0 370.18 0.35 $ Top Left Tie Rod
1044 rcc  3.36 6.72 0 0 0 370.18 0.28 $ Top Right Tie Rod
```

```
1045 rcc  3.36 6.72 0 0 0 370.18 0.35 $ Top Right Tie Rod
1046 rcc −1.68 1.68 0 0 0 370.18 0.28 $ Top Left Tie Rod
1047 rcc −1.68 1.68 0 0 0 370.18 0.35 $ Top Left Tie Rod
1048 rcc  3.36 1.68 0 0 0 370.18 0.28 $ Top Right Tie Rod
1049 rcc  3.36 1.68 0 0 0 370.18 0.35 $ Top Right Tie Rod
c ========= Spacers ==========
1050 rcc  0.84 4.2 27.5 0 0 2 5.8  $ First Spacer
1051 rcc  0.84 4.2 56 0 0 2 5.8    $ Second Spacer
1052 rcc  0.84 4.2 84.5 0 0 2 5.8  $ Third Spacer
1053 rcc  0.84 4.2 113 0 0 2 5.8   $ Fourth Spacer
1054 rcc  0.84 4.2 141.5 0 0 2 5.8 $ Fifth Spacer
1055 rcc  0.84 4.2 170 0 0 2 5.8   $ Sixth Spacer
1056 rcc  0.84 4.2 198.5 0 0 2 5.8 $ Seventh Spacer
1057 rcc  0.84 4.2 227 0 0 2 5.8   $ Eigth Spacer
1058 rcc  0.84 4.2 255.5 0 0 2 5.8 $ Ninth Spacer
1059 rcc  0.84 4.2 284 0 0 2 5.8   $ Tenth Spacer
1060 rcc  0.84 4.2 312.5 0 0 2 5.8 $ Eleventh Spacer
1061 rcc  0.84 4.2 341 0 0 2 5.8   $ Twelvth Spacer


c ========= Data Card ==========
MPHYS ON
ACT DN=MODEL
KCODE 10000 1.0 50 150
KSRC −1.68 8.4 50 0 8.4 50 1.68 8.4 50 3.36 8.4 50 −3.36 6.72
    50 &
        0 6.72 50 1.68 6.72 50 5.04 6.72 50 −3.36 5.04 50
            −1.68 5.04 50 &
```

0 5.04 50 1.68 5.04 50 3.36 5.04 50 5.04 5.04 50
−3.36 3.36 50 &
−1.68 3.36 50 0 3.36 50 1.68 3.36 50 3.36 3.36 50
5.04 3.36 50 &
−3.36 1.68 50 0 1.68 50 1.68 1.68 50 5.04 1.68 50
−1.68 0 50 &
0 0 50 1.68 0 50 3.36 0 50 −1.68 8.4 200 0 8.4 200
1.68 8.4 200 &
3.36 8.4 200 −3.36 6.72 200 0 6.72 200 1.68 6.72 200
5.04 6.72 200 &
−3.36 5.04 200 −1.68 5.04 200 0 5.04 200 1.68 5.04
200 3.36 5.04 200 &
5.04 5.04 200 −3.36 3.36 200 −1.68 3.36 200 0 3.36
200 1.68 3.36 200 &
3.36 3.36 200 5.04 3.36 200 −3.36 1.68 200 0 1.68 200
1.68 1.68 200 &
5.04 1.68 200 −1.68 0 200 0 0 200 1.68 0 200 3.36 0
200 −1.68 8.4 350 &
0 8.4 350 1.68 8.4 350 3.36 8.4 350 −3.36 6.72 350 0
6.72 350 &
1.68 6.72 350 5.04 6.72 350 −3.36 5.04 350 −1.68 5.04
350 0 5.04 350 &
1.68 5.04 350 3.36 5.04 350 5.04 5.04 350 −3.36 3.36
350 −1.68 3.36 350 &
0 3.36 350 1.68 3.36 350 3.36 3.36 350 5.04 3.36 350
−3.36 1.68 350 &

```
        0 1.68 350 1.68 1.68 350 5.04 1.68 350 -1.68 0 350 0
          0 350 1.68 0 350 &
        3.36 0 350
c ======== BURN Paremeters ==========
BURN Time=1095 PFRAC=1 POWER=2.487 MAT=1 2 4 5 BOPT=1.0 24 1
  &
       MATVOL=16872.31 4492.1 6432.78 1151.27
c ======== Material Card ==========
m1  92235 -0.006221 92238 -0.868695 8016 -0.118467 &
       94239 -0.003838 94240 -0.001588 94241 -0.000926 &
       94242 -0.000255 $MOX Fuel
m2  24050 -0.004 24052 -0.084 24053 -0.010 &
       24054 -0.002 26054 -0.006 26056 -0.092 &
       26057 -0.002 26058 -0.0003 28058 -0.034 &
       28060 -0.013 28061 -0.001 28062 -0.002 &
       28064 -0.0005 8016 -0.120 50000 -1.400 40000 -98.23
          $Zirc2
m3  1001 2.0 8016 1.0 $ Light water
mt3 lwtr
m4  41093 -2.5 40000 -97.5 $Zr-2.5w/o Nb
m5  6000 -0.08 14000 -0.35 15031 -0.015 16032 -0.015 24050
  -0.793 &
       24052 -15.903 24053 -1.838 24054 -0.466 25055 -0.35
          26054 -0.958 &
       26056 -15.442 26057 -0.36 26058 -0.049 28058 -35.382
          28060 -13.993 &
```

```
        28061 -0.616 28062 -1.989 28064 -0.52 5010 -1.078E-3
           &
        5011 -4.925E-3 22000 -0.9 13027 -0.5 27059 -1 29063
           -0.205 &
        29065 -0.095 41093 -2.563 42000 -3.05 73181 -2.563
           $Inconel-718
print
```